

**Best
Available
Copy**

AD-A143 928



(2)

Report

THREE-DIMENSIONAL PHOTOCHEMICAL
MACHINING WITH LASERS

to

U.S. AIR FORCE
OFFICE OF SCIENTIFIC RESEARCH

November 30, 1983

ADVANCED RESEARCH PROJECTS AGENCY (DOD)

Approved for public release
Distribution unlimited

FIRST ANNUAL TECHNICAL REPORT

on

**AIR FORCE OFFICE OF SCIENTIFIC RESEARCH (AFOSR)
NOTICE OF TRANSMITTAL TO DTIC**

This technical report has been reviewed and is approved for public release IAW AFM 190-12. Distribution is unlimited.

MATTHEW J. KERPER

Chief, Technical Information Division

**THREE-DIMENSIONAL PHOTOCHEMICAL
MACHINING WITH LASERS**

to

**U.S. AIR FORCE
OFFICE OF SCIENTIFIC RESEARCH**

November 30, 1983

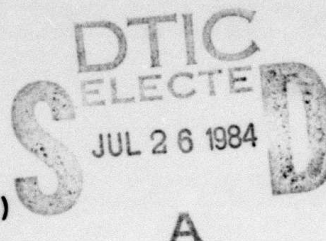
ADVANCED RESEARCH PROJECTS AGENCY (DOD)

ARPA Order No. 4522, Program Code 2D10

Monitored by AFOSR Under Contract No. F49620-82-C-0077

Principal Investigator: Robert E. Schwerzel
**Project Team Members: William A. Ivancic, Vincent D. McGinniss,
Van E. Wood, and Carl M. Verber**
**Project Consultants: Jerry A. Jenkins, Steven Kramer, and
Wyn Kelly Swainson**

**BATTELLE
Columbus Laboratories
505 King Avenue
Columbus, OH 43201**



UNCLASSIFIED

SECURITY CLASSIFICATION OF THIS PAGE (When Data Entered)

REPORT DOCUMENTATION PAGE		READ INSTRUCTIONS BEFORE COMPLETING FORM
1. REPORT NUMBER AFOSR-PR-84-0587	2. GOVT ACCESSION NO. AD-A143928	3. RECIPIENT'S CATALOG NUMBER
4. TITLE (and Subtitle) Three-Dimensional Photochemical Machining with Lasers		5. TYPE OF REPORT & PERIOD COVERED Annual Technical Report (6/1/82-6/30/83)
		6. PERFORMING ORG. REPORT NUMBER
7. AUTHOR(s) Dr. Robert E. Schwerzel		8. CONTRACT OR GRANT NUMBER(s) F49620-82-C-0077
9. PERFORMING ORGANIZATION NAME AND ADDRESS Battelle, Columbus Laboratories 505 King Avenue Columbus, Ohio 43201		10. PROGRAM ELEMENT, PROJECT, TASK AREA & WORK UNIT NUMBERS 601102F, DARPA
11. CONTROLLING OFFICE NAME AND ADDRESS Defense Advanced Research Projects Agency Materials Sciences Division 1400 Wilson Blvd., Arlington, VA 22209		12. REPORT DATE November 30, 1983
		13. NUMBER OF PAGES 83
14. MONITORING AGENCY NAME & ADDRESS (if different from Controlling Office) Air Force Office of Scientific Research Directorate of Electronic & Materials Science Building 410 Bolling AFB, DC 20332		15. SECURITY CLASS. (of this report) Unclassified
		15a. DECLASSIFICATION/DOWNGRADING SCHEDULE None
16. DISTRIBUTION STATEMENT (of this Report) Unrestricted Approved for public release; distribution unlimited		
17. DISTRIBUTION STATEMENT (of the abstract entered in Block 20, if different from Report)		
18. SUPPLEMENTARY NOTES		
19. KEY WORDS (Continue on reverse side if necessary and identify by block number) Photochemical Machining, Lasers, Polymers, Photoinitiators, Porphyrins		
20. ABSTRACT (Continue on reverse side if necessary and identify by block number) Research on the development of new photoinitiator systems for spatially selective photochemical machining with lasers has continued smoothly and is progressing well. The porphyrin system developed during the first quarter continues to look particularly promising. A number of potential new candidate materials have also been identified, including a rubrene sulfonyl chloride derivative. Experimental study of these new compounds was begun during the past quarter and is expected to continue for several more months. Detailed calculations		

DD FORM 1 JAN 73 1473

EDITION OF 1 NOV 65 IS OBSOLETE

UNCLASSIFIED

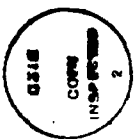
SECURITY CLASSIFICATION OF THIS PAGE (When Data Entered)

UNCLASSIFIED

SECURITY CLASSIFICATION OF THIS PAGE(When Data Entered)

20.

have also been carried out to relate optical and materials parameters to the overall efficiency of the photochemical machining process, and a new optical design has been conceived. Future work will concentrate heavily on the evaluation of suitable polymer systems for the fabrication of three-dimensional objects having good surface finish and mechanical stability.



Access	<input checked="" type="checkbox"/>
NTIS	<input type="checkbox"/>
DISSEM	<input type="checkbox"/>
U	
J	
F	
100 5	
/or	
Dist	
A-1	

UNCL

SECURITY CLASSIFICATION OF THIS PAGE(When Data Entered)

EXECUTIVE SUMMARY

The fabrication of objects having complex, three-dimensional shapes frequently requires a substantial expenditure of time, labor, and capital. This is particularly true of manufacturing techniques such as investment casting, where a wax or plastic replica of the finished object must be made before an actual metal casting can be produced. Because this process necessarily employs much skilled hand labor, many weeks or months may be required to proceed from design specifications to a prototype casting. Clearly, much cost and effort could be saved if it were possible to fabricate a complex plastic pattern directly from design data without the intermediacy of a hand-made metal mold or die.

The research program described in this report has been designed to evaluate a novel, and as yet undeveloped, technology which has the potential to revolutionize the casting industry. The key to this new technology, which may be referred to as "Photochemical Machining", or PCM, is the computer-assisted fabrication of a plastic pattern directly from design specifications, by the selective, three-dimensional modification of a plastic material which is exposed simultaneously to two different laser beams which are focused onto a single point within the volume of the material.

If the chemical composition of a plastic material were designed properly, the solubility and hardness of the plastic could, in principle, be altered selectively at the point of intersection of the two beams without being affected by either beam alone. Given such a material, a three-dimensional object of any desired complexity could be fabricated directly by appropriate movements of the two laser beams (and thus of the intersection point) throughout the volume of the material. The softer, more soluble portions of the plastic could then be removed selectively, leaving a hard, rigid plastic piece having the desired shape.

Ideally, this piece would be suitable for immediate use for investment casting, electroplating, and so on, with minimal finishing being required. In this way, for example, prototype designs could easily be subjected to "real-world" test conditions and then modified easily and inexpensively by repeating the PCM process described above as often as

needed to fully optimize the design. This could result in dramatic savings of time, labor, and cost. In addition, the complete three-dimensional flexibility provided by the PCM concept could lead to the casting of complex shapes which are at present difficult to fabricate, and make possible the production of precise castings which require minimal subsequent machining or finishing.

The research conducted during the past year has been successful in developing a theoretical framework for relating optical and materials properties to the performance of a PCM system, and in designing and synthesizing several novel photosensitive compounds whose spectroscopic properties make them attractive candidates for use in a PCM system. These compounds are capable of initiating polymerization when they are irradiated with light beams of two different wavelengths, but not with either wavelength alone.

Battelle's experiments to date have been conducted with solutions of the candidate photoinitiators in liquid methyl methacrylate, for reasons of experimental convenience; the amount of polymer formed has been measured by simply precipitating the resulting polymer with methanol and weighing it. While this approach has worked well for screening a variety of potential photoinitiators, it is obviously unsatisfactory for the production of three-dimensional objects. For this reason, the research to be performed during the coming year will be directed toward the evaluation of novel polymer compositions containing these photoinitiators that will be capable of rapid crosslinking to provide a hard, insoluble, three-dimensional object with good surface finish and mechanical stability. This work will provide a demanding test of the commercial viability of the photochemical machining concept.

TABLE OF CONTENTS

	<u>Page</u>
EXECUTIVE SUMMARY	i
INTRODUCTION	1
Description of the Photochemical Machining Concept	4
Possible Modes of Operation	5
Anticipated Benefits of a PCM System	7
Background Information	8
Program Objectives	9
RESULTS AND DISCUSSION	10
Theoretical Considerations	10
Design of New Photoinitiator Molecules	20
Photoinduced Crosslinking of Polymers	34
Photophysical Processes	39
Mechanisms For Photochemical Production of	
Free Radical Intermediates	41
Photopolymerization	46
Polymeric Crosslinking Reactions	49
Two-Photon Triplet Sensitized Photopolymerization	
Using Dibromoanthracene and	
Naphthalenesulfonylchloride	53
Experimental Details	59
Key Observations	60
Two-Photon Laser Studies	63
Experimental Design	65
Experimental Results and Expected	
Direction of Research	70
Estimated Amount of Polymerization Expected	
from Two-Beam Laser Experiments	71
SUMMARY OF FUTURE PLANS	77
REFERENCES.	79

LIST OF FIGURES

FIGURE 1.	SCHEMATIC ILLUSTRATION OF A COMPUTER-ASSISTED PHOTOCHEMICAL MACHINING (PCM) SYSTEM	4
FIGURE 2.	ONE POSSIBLE MOLECULAR ENERGY-LEVEL DIAGRAM FOR PRODUCTION OF INITIATOR SPECIES FOR CHAIN EXTENSION OR CROSS-LINKING OF POLYMERS	12
FIGURE 3.	GENERAL STRATEGY FOR PHOTOINITIATOR DESIGN	21
FIGURE 4.	ABSORPTION SPECTRA OF p-SUBSTITUTED BENZOPHENONE DERIVATIVES	38
FIGURE 5.	SCHEMATIC JABLONSKI DIAGRAM FOR A TYPICAL ORGANIC MOLECULE	39
FIGURE 6.	TIME SEQUENCE OF A TYPICAL VINYL POLYMERIZATION REACTION	49
FIGURE 7.	ENERGY-LEVEL DIAGRAM FOR 9,10-DIBROMOANTHRACENE . . .	54
FIGURE 8.	SCHEMATIC ENERGY-LEVEL DIAGRAM FOR TRIPLET- SENSITIZED EXCITATION OF DIBROMOANTHRACENE	59
FIGURE 9.	EXPERIMENTAL ABSORPTION SPECTRA FOR DBA AND FOR NSC IN METHYL METHACRYLATE, SHOWING TRANSMISSION CURVE FOR CORNING CS 3-74 FILTER	61
FIGURE 10.	PHOTOPOLYMER FORMATION IN THE DBA/NSC/MMA SYSTEM. . .	62
FIGURE 11.	ILLUSTRATION OF TWO-BEAM LASER IRRADIATION SYSTEM . .	66
FIGURE 12.	SCHEMATIC ILLUSTRATION OF LASER TRIGGERING SCHEME . .	69
FIGURE 13.	VIEWS OF FOCUSED BEAM INTERSECTIONS	74

LIST OF TABLES

TABLE 1.	SUMMARY OF SPECTROSCOPIC DATA	23
TABLE 2.	TRIPLET-TRIPLET ABSORPTION SPECTRA OF CARBONYL COMPOUNDS.	24
TABLE 3.	TRIPLET-TRIPLET ABSORPTION SPECTRA OF ORGANIC DYESTUFFS	27
TABLE 4.	MOLECULAR STRUCTURE-EXTINCTION COEFFICIENT RELATIONSHIPS	37
TABLE 5.	MOLECULAR STRUCTURE-TRIPLET ENERGY RELATIONSHIPS . . .	41

TABLE OF CONTENTS
(Continued)

	<u>Page</u>
TABLE 6. SUMMARY OF DBA/NSC IRRADIATION EXPERIMENTS	64
TABLE 7. DATA ON LASERS AND MATERIALS INTERACTIONS USED IN TWO-PHOTON EXPERIMENTS ON POLYMERIZATION OF METHYL METHACRYLATE WITH PORPHYRIN SENSITIZATION. . . .	68

FIRST ANNUAL TECHNICAL REPORT

on

THREE-DIMENSIONAL PHOTOCHEMICAL
MACHINING WITH LASERS

to

U.S. AIR FORCE
OFFICE OF SCIENTIFIC RESEARCH

from

BATTELLE
Columbus Laboratories

November 30, 1983

INTRODUCTION

The production of castings having complex, three-dimensional shapes is so commonplace in today's technology that the enormous amount of painstaking manual effort involved is easily overlooked. Skilled artisans must labor for days or months to transform a set of blueprints and specifications into a "real" object, or to create the dies used to fabricate stamped or molded objects. Similarly, the duplication of an existing object may require the production of a mold from which a replica can be cast, or the fabrication of a replica by hand. While the gradual introduction of computer-assisted design and manufacturing techniques has increased the speed and flexibility of certain processes, a great deal of manual, artistic skill is still required. Furthermore, many of the potential advantages of computer-assisted design and manufacturing are lost because of the intrinsic limitations of the conventional manufacturing techniques to which the computer is applied.

Conventional manufacturing technology requires not only the use of multiple tools--lathes for the generation of cylindrical ribbed or round forms, drills for holes, milling machines for flat surfaces, and so on, but it requires also the application of great force for the removal or displacement of the material being worked. And it combines this need for force with the need for precision.

Even where advanced numerical control (NC) techniques are used, great inefficiency occurs in the course of proceeding from original design concepts through blueprinting or other design documentation, to model-making and the preparation of NC control tapes or programs specifying the semiautomatic sequence of operations on separate lathes, milling machines, drills, and the like which are required to fabricate a finished piece.

Clearly, much time, effort, and expense could be saved if the capabilities of the computer could be used to assist in the production of three-dimensional phototypes directly in the design and fabrication stages. The same techniques could permit the replication of objects in nearly any desired size, given a computer-compatible description of the original. For instance, such diverse objects as automotive or aircraft parts, models for wind-tunnel tests, intricate three-dimensional models for architecture or structural engineering design studies, or prototype artificial prosthetic devices could all be described by the appropriate computer-compatible notation, and the design features optimized as much as possible by computer calculations. If the computer could then control directly the production of a prototype object, utilizing the optimized design parameters, the design could be evaluated immediately by examination or by experimental means. Given the appropriate computerized description, entire complex clusters, made of disposable pattern material and ready for casting, could be automatically generated, tested, and then remade by simple changes in the computer program for the correction of gates and sprue routing, proportion, size, quantity, and the like.

In such a system, there would be direct and efficient interaction between the design engineer and the actual manipulable object gener-

ated. The effect would be as though the design and manufacturing system operated as a perfectly flexible machine tool, capable of creating an infinite choice of complex shapes -- carburetor housings, gears, turbine blades, anthropomorphic forms, reentrant-shaped surfaces or holes, and so on.

It is the purpose of this report to describe the results of Battelle's efforts to date in evaluating and developing a novel concept which could form the basis for truly implementing the futuristic technology envisioned above. The key to this new concept, which may be referred to as "Photochemical Machining", or PCM, is the computer-assisted fabrication of a plastic pattern directly from design specifications by the selective, three-dimensional modification of a plastic material which is exposed simultaneously to two laser beams focused onto a single point within the volume of the material. If the chemical composition of the plastic is designed properly, the solubility and hardness of the plastic can, in principle, be altered selectively at the point of intersection of the two beams without being affected by either beam alone.

Given such a material, a three-dimensional object of any desired complexity could be fabricated directly by appropriate movements of the two laser beams (and thus of the intersection point) within the volume of the material. The softer, more soluble portions of the plastic could then be removed selectively by a variety of means, leaving a hard, rigid plastic piece having the desired shape. This piece could then be used directly for investment casting, electroforming, or other end-use applications, as desired.

While the PCM concept as summarized above seems in some respects to be particularly well suited to investment casting by "lost wax" techniques, in Battelle's view this new technology could provide major benefits to all facets of the casting industry and could, if fully developed and exploited, bring about a major change in the way manufacturing technology is perceived and practiced today.

Description of the Photochemical Machining Concept

The essential features of a conceptual PCM system for the computer-assisted photochemical fabrication of three-dimensional precision patterns are depicted in Figure 1. As mentioned above, the pattern is formed from a polymer which can either be photochemically crosslinked

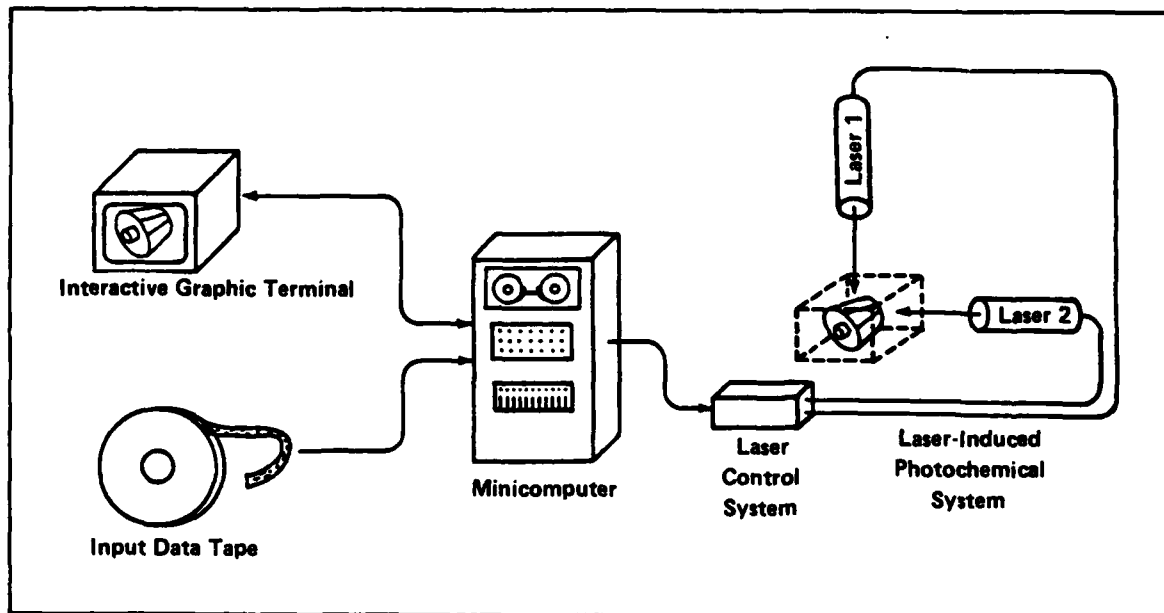


FIGURE 1. SCHEMATIC ILLUSTRATION OF A COMPUTER-ASSISTED PHOTOCHEMICAL MACHINING (PCM) SYSTEM

(made hard and insoluble) or degraded (made soft and easily dissolved or vaporized), depending on its chemical composition, by simultaneous exposure to the intersecting laser beams. In effect, the point of intersection of the laser beams serves as an highly flexible machine tool; because

the formation of the plastic pattern is achieved by means of photochemical reactions which occur only at the intersection point, the speed and efficiency of the process are affected only slightly by the complexity of the shape being produced.

In this conceptual PCM system, the minicomputer accepts input describing the size and shape of the object to be made, either from an interactive graphic terminal (which allows the operation the flexibility of drawing and modifying the design before a solid object is made) or from previously recorded data obtained elsewhere. It then generates the set of coordinates which will control the actual pattern-forming process. Such computerized input and data processing systems have been dramatically improved during the past several years; for example, Battelle has developed an interactive, computer-controlled milling machine based on such technology. Thus, the essential computer techniques already exist, for the most part, and relatively little effort should be required to upgrade them for use with the proposed PCM system.

Possible Modes of Operation

Depending on the properties of the polymer system and the requirements of the object to be formed, the PCM system can, in principle, be designed to operate in either of two modes:

- "Synthetic" Mode - In this mode, a rigid, crosslinked, insoluble polymer is formed by the photochemical crosslinking of a soluble, low molecular weight polymer precursor. The finished pattern is then "freed" by dissolving or vaporizing the uncrosslinked precursor.
- "Sculpting" Mode - In this mode, which is the converse of the synthetic mode, the precursor is a rigid, crosslinked poly-

mer. The unwanted polymer is degraded at the reaction point, leaving the desired object unchanged; the degraded polymer may then be dissolved or vaporized, as above.

In both cases, the photochemical reactions which result in the formation of the object must occur only at the reaction point, and not in either beam alone. To achieve this, the chemical composition of the plastic must be designed in such a way that two photons (particles of light) are required to initiate the key photochemical reactions. A number of photochemical materials are amenable to this two-photon approach, and the choice of the reactions actually used will depend heavily on the properties desired in the final pattern. In general, however, the photochemical reactions will rely on the sequential absorption of two photons by the plastic material. The first photon will produce a reactive intermediate chemical species, and the second will cause an irreversible photochemical reactions of that intermediate. As the reactive intermediate will in general have absorption properties quite different from those of the precursor, there will be little chance of having the reaction occur in the presence of either beam alone. Thus, one laser beam will be of a color absorbed strongly by the original material, while the second beam will be of a color which is absorbed strongly by the reactive intermediate. As mentioned above, it is anticipated that the uncrosslinked portions of the plastic material will be removed either by washing the pattern with an appropriate solvent or by vaporizing the material, leaving behind the hard, rigid plastic pattern. Note that the entire volume of the pattern need not be fully polymerized; it may be sufficient to simply harden a shell with a few internal supports in key locations.

While many of the components required for PCM have been developed to a significant extent, the commercial feasibility of developing an operational PCM system has not yet been demonstrated. It remains to fully evaluate the chemical and optical constraints on the operation of a PCM system, to develop and optimize the various system components which will be required, and to construct and evaluate a fully operational device which will be suitable for the fabrication of patterns for precision

casting applications. Our research effort in this program has been directed toward these goals.

Anticipated Benefits of a PCM System

We envision that a PCM system, once developed, would offer its users significant benefits in speed, convenience, precision, and cost as compared to conventional techniques. The novel capabilities which a PCM system would offer include the following:

- Rapid Computer-Assisted Fabrication. The fabrication of the plastic pattern would be accomplished under computer control, using coordinates generated by the computer from the optimized design information. This would eliminate much of the costly, time-consuming hand labor which is now required for the fabrication of patterns, and could reduce the time required to produce a prototype casting from several months to several days or less.
- Design Optimization. Through the use of interactive input, the user could, if desired, design optimized shapes for a variety of cast metal or plastic objects, using the computer and the PCM system to fabricate prototype castings which could then be evaluated under actual test conditions. This process would avoid much of the time-consuming manual trial-and-error process currently involved in the design and fabrication of prototype cast parts, particularly for those parts which can be made by investment casting techniques. The application of the PCM concept to investment casting seems particularly attractive in this context, as in principle the plastic piece could be used directly in a "lost wax" process.

- Precise Scaling. The size of the objects produced could be scaled up and down easily by adjusting the output parameters of the computer control system.
- Reduced Need for Subsequent Machining. The objects produced will be hard, dry, and ready for examination, plating, or other uses as desired. In addition, because of the ease with which a PCM system will be able to fabricate complex shapes, it should be possible to produce castings with complex curvatures, internal holes or structures, and even prethreaded holes for screws or other fittings. Thus, castings produced by the PCM method should require less subsequent machining than those produced by conventional techniques.

Background Information

The concept for photochemical machining described above has its origins in research performed independently during the past decade by scientists at Battelle's Columbus Laboratories and at the Formigraphic Engine Corporation, a small company located in Oakland, California. The original patent application, which describes all of the essential features of a PCM system, was filed in 1967 by Mr. W. K. Swainson, now president of the Formigraphic Engine Corporation and a consultant to Battelle for this research program. This was followed by other patent applications by Mr. Swainson which described specific components and applications of the PCM concept in more detail. Meanwhile, scientists at Battelle's Columbus Laboratories independently filed patent applications describing their work on a three-dimensional real-time fluorescent display system (that is, a "3-D oscilloscope"). This research involved the use of intersecting light beams to produce an isolated fluorescent spot, which could be moved in three dimensions as the point of intersection of the beams was moved. Thus, the 3-D fluorescent display system encompassed many of the concepts which are implicit in photochemical machining.

These patent applications eventually led to the issuance of U.S. Patents 3,609,706 and 3,829,838 to Battelle, and U.S. patents 4,041,476 and 4,078,229 to the Formigraphic Engine Corporation. The Formigraphic patents may have priority over many of the claims in the Battelle patents, by virtue of their earlier filing date.

While this research and development program is being conducted at Battelle's Columbus Laboratories, Formigraphic Engine Corporation is assisting Battelle in a consulting capacity. Because PCM technology is still very much in the formative stages, a relatively large research effort may be required to bring the PCM concept to commercialization if the results of the proposed feasibility evaluation indicate that such effort is warranted. Battelle would therefore welcome the participation of industrial co-sponsors in sharing the costs and benefits of this effort, so as to assist the Government in the transfer of this new technology to the industrial sector.

Program Objectives

The principal objectives of this research program are:

- To evaluate in detail the technical feasibility of developing a photochemical machining (PCM) system suitable for the fabrication of patterns for precision casting applications, and
- To develop the individual chemical and optical components which will be required to evaluate realistically the feasibility of a prototype PCM system.

These objectives are directed toward conducting the evaluation of PCM technology as efficiently as possible, and toward providing AFOSR with a logical progression of decision points by which the progress of the project can be evaluated in the context of DOD's own interests and constraints. The results which have been obtained during the past year's research effort described in the following sections of this report.

RESULTS AND DISCUSSION

Theoretical Considerations

In any practical photochemical machining system, there are obviously numerous design tradeoffs among such factors as laser power, workpiece size, surface finish, and fabrication time to be considered. It is helpful to work through a simple model of the system at the outset, in order to get a general idea of what the tradeoffs are, and of what is going to be required of the chemicals for the system to have a chance to work. We describe such a model calculation in this section.

Let us consider, for the sake of definiteness, a cubical sample volume, 10 cm on a side. Within this volume, we wish to be able to address spots 10 μm on a side with orthogonally propagating laser beams. These numbers are consistent with present-day beam-shaping and scanning equipment. The sample volume thus contains 10^{12} addressable spots. To produce a useful item, say a release mold outline, let us assume that we have to polymerize 10% of the sample volume, or, roughly, that we have to produce polymer in 10^{11} spots forming a connected surface and nowhere else.

We will assume that the polymer is produced by chain extension, cross-linking, or some similar process, stimulated by the presence of some photoproduct "initiator" molecular species. We will not focus on the details of the polymerization process, but rather will simply consider as

one goal of the calculation an estimate of the amount of polymerization required per significant photochemical event. One possible molecular-energy-level model for the initiator part of the process is shown in Figure 2. In this representation, straight arrows indicate radiative transitions, and wavy arrows indicate primarily non-radiative transitions (although D_S and D_T include a small spontaneous radiation component). The singlet ground state of a "sensitizer" molecule is pumped by the first laser beam to the excited state S_1 . Some of the S_1 -state molecules decay nonradiatively to the metastable triplet state T_1 . Molecules in this state are pumped by the second, orthogonal, laser beam to the excited state T_x , from which some of them can react with each other or with other species present in solution to form the initiator species indicated schematically on the diagram at the level P.

The transfer rates indicated in Figure 2 are identified as follows: A_S is the rate at which molecules are excited from the ground-state level S_0 to S_1 ; it equals $I_1 \sigma_S$, where I_1 is the intensity (photons per unit area per second) of laser beam 1 and σ_S is the cross-section for the absorption process at the wavelength of beam 1. The stimulated decay rate from S_1 is indicated as A_S' ; since the molecular excited state will generally be structurally altered from the ground state, the Einstein relations do not necessarily hold; that is, A_S' is not necessarily equal to A_S . In the calculations, we have assumed that stimulated decays from S_1 and T_x can both be neglected; trial calculations including them show that this is a very good approximation. D_S represents the combined rate of nonradiative and spontaneous radiative decay processes from S_1 to S_0 , while Q_T is the rate of transfer from S_1 to the lowest triplet level T_1 . The transfer rates for the triplet-state processes are defined in a similar way, except that Q_p is the rate of production of initiator species. As indicated on the diagram, decay rates from the lowest triplet state to the ground state are assumed to be slow; the associated time constants will be milliseconds or longer, so these processes can be ignored in the dynamic analysis.

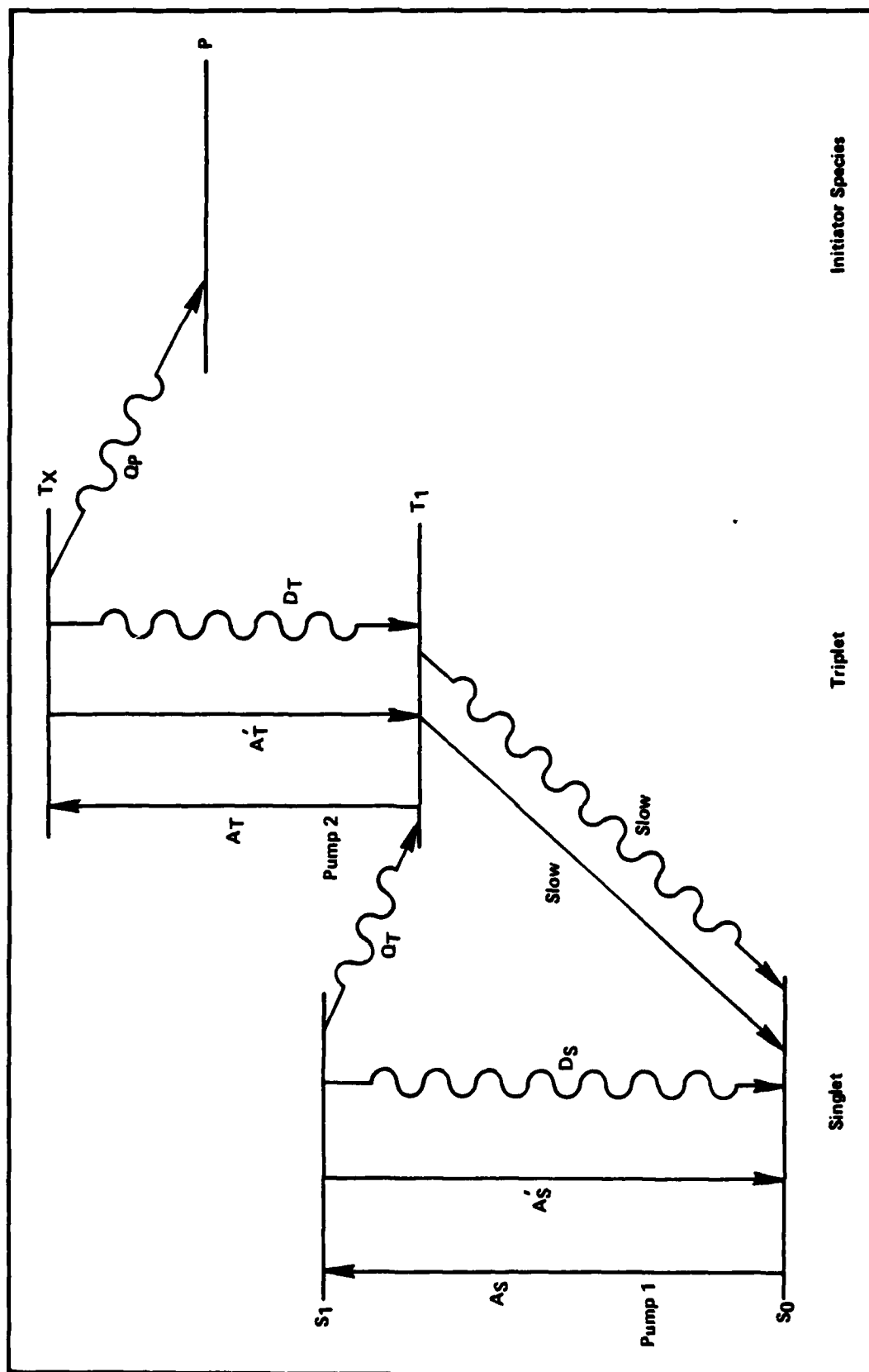


FIGURE 2. ONE POSSIBLE MOLECULAR ENERGY-LEVEL DIAGRAM FOR PRODUCTION OF INITIATOR SPECIES FOR CHAIN EXTENSION OR CROSS-LINKING OF POLYMERS

With these definitions and assumptions given, it is now easy to write down the rate equations describing the model system:

$$dn_{S_0}/dt = -A_S n_{S_0} + D_S n_{S_1} ; \quad (1)$$

$$dn_{S_1}/dt = A_S n_{S_0} - (D_S + Q_T) n_{S_1} ; \quad (2)$$

$$dn_{T_1}/dt = Q_T n_{S_1} - A_T n_{T_1} + D_T n_{T_x} ; \quad (3)$$

$$dn_{T_x}/dt = A_T n_{T_1} - (D_T + Q_P) n_{T_x} ; \quad (4)$$

$$dn_P/dt = Q_P n_{T_x} . \quad (5)$$

In these equations, n_{S_0} indicates the number of molecules per unit volume in state S_0 , and so forth. The initial conditions may be taken to be

$$n_{S_0}(0) = N_S , \quad (6)$$

where N_S is of course the initial concentration of sensitizer molecules, with all other states initially empty.

It is possible to give a general solution to this system of equations, but such a solution is fairly complicated and not really necessary for the present first-cut model calculations. Rather, we will introduce some additional assumptions which simplify the physical picture while neither leading to any unwarranted mathematical approximations nor involving unlikely physical embodiments of the apparatus.

First, we shall assume that the singlet and triplet pumps are at decidedly different wavelengths, so that neither absorption process substantially affects the other. This situation should not be too difficult to obtain experimentally, although there may be a tradeoff to consider between broader absorption bands, more likely to have useful absorption

coefficients at available laser wavelengths, and narrower absorption bands, less likely to overlap.

Second, we limit the discussion to the case of sequential excitation, in which the singlet pump laser 1 is turned on for a time τ_1 and then turned off while the triplet pump laser is turned on for a time τ_2 . This assumption simplifies the mathematics while being very conservative in regard to attainable operating conditions.

Third, we simplify the boundary conditions by neglecting the small number of molecules transferred from S_1 to T_1 after beam 1 is turned off, and by neglecting the depletion of the ground state. Although a number of cycles of sequential excitation might be necessary fully to polymerize a given location, the calculations will show that the ground-state depletion is insignificant. Neglecting the singlet-triplet transfer after beam 1 is extinguished is again a "conservative" or worst-case assumption.

With these assumptions, solution of the rate equations (1)-(5) degenerates into the solution of two independent and formally identical simple problems, one represented by the first two equations and the other by the last three. The right-hand side of Eq. (3) contains only the first term while the singlet pump is active, and only the other two terms when the triplet pump is on. We have solved these equations by the Laplace transform method. The results have the considerable advantage that they are simple enough in form that it is not difficult to see how changes in the various parameters affect the rate of initiator molecule production. As is usual in such circumstances, the same combinations of parameters recur frequently in the results; so it is helpful to introduce some notation for these combinations.

First we introduce in the usual way the overall decay times characterizing the excited states:

$$\tau_S = (D_S + Q_T)^{-1} ; \quad (7)$$

$$\tau_T = (D_T + Q_p)^{-1} . \quad (8)$$

In terms of these decay times, we can define the fractional intersystem transfer probabilities by

$$f_S = Q_T \tau_S ; \quad (9)$$

$$f_T = Q_p \tau_T . \quad (10)$$

Similarly, we can define fractional excitation-to-decay ratios for each subsystem by

$$G_S = A_S \tau_S ; \quad (11)$$

$$G_T = A_T \tau_T . \quad (12)$$

Normalized illumination times are defined by

$$\rho_S = \tau_1/2 \tau_S ; \quad (13)$$

$$\rho_T = \tau_2/2 \tau_T . \quad (14)$$

Other parameters which appear frequently are

$$R_S = [(1+G_S)^2 - 4F_S G_S]^{1/2} \quad (15)$$

and R_T which is defined similarly. Finally, we define N_T as the number of sensitizer molecules per unit volume transferred to the T_1 state after one cycle of the singlet-state pump, and N_p as the number of these molecules transferred to the initiator state P after one cycle of each pump. We will denote by N_S^* the number of sensitizer molecules left in the ground state after the singlet-state pump cycle.

Then, in terms of the dimensionless variables we have defined, the fractions of sensitizer molecules left in the ground state, transferred to the lowest triplet state, and transferred to the initiator configuration, per cycle of singlet-state and triplet-state pump in a given location, are given by Equations 16-18 as follows:

$$\frac{N_S^*}{N_S} = \frac{1}{2R_S} \left[(1-G_S + R_S)e^{-(1G_S-R_S)\rho_S} - (1-G_S-R_S)e^{-(1+G_S+R_S)\rho_S} \right] ; \quad (16)$$

$$\frac{N_T}{N_S} = \frac{2F_S G_S}{R_S} \left[\frac{1-e^{-(1+G_S-R_S)\rho_S}}{1+G_S-R_S} - \frac{1-e^{-(1+G_S+R_S)\rho_S}}{1+G_S+R_S} \right] ; \quad (17)$$

and

$$\frac{N_p}{N_T} = \frac{2F_T G_S}{R_T} \left[\frac{1-e^{-(1+G_T-R_T)\rho_T}}{1+G_T-R_T} - \frac{1-e^{-(1+G_T+R_T)\rho_T}}{1+G_T+R_T} \right] ; \quad (18)$$

respectively.

To evaluate these expressions, it is necessary to make more specific assumptions about the system. Suppose we aim for a total laser-beam dwell time at each addressed spot of one μsec . Then to polymerize 10^{11} points will require 10^5 seconds, or a little over a day, neglecting the time for moving the beams around.

Next we should consider desirable attenuation characteristics of the beams. The singlet-state pump absorption should be moderate, so that reduction of available intensity at remote points in the sample does not result in a requirement of greatly increased exposure times at these points. If for instance the power attenuation coefficient $\alpha_S = 0.2 \text{ cm}^{-1}$, then a beam at the center of the sample is attenuated by a factor of $1/e$, or 0.36, which should be tolerable. We shall assume we can adjust the singlet-pump attenuation to something like this value. The triplet-state absorption should of course be as high as possible in order to maximize the transfer to initiator states.

To relate the absorption coefficients to the parameters previously defined, we recall that

$$\sigma_S = \alpha_S / N_S ; \quad (19)$$

so that

$$G_S = I_1 \alpha_S \tau_S / N_S , \quad (20)$$

and similarly for G_T . In evaluating these expressions, we have naturally assumed that the molecular-species densities in the denominator do not change during the operative cycle time, since σ is the fundamental physical parameter and since the absorption coefficients are measured when the lower states are well-populated. Since the singlet-state absorption coefficient is low, the corresponding laser power must be large, even if the larger part of the dwell period is devoted to the ground state excitation. Suppose we take the singlet state pump as the 514.5 nm line of an argon laser, and assume that we can devise a molecule with suitable absorption at this wavelength. Suppose the laser power is 20 W, not out of the question with present-day equipment, and let us take this power to be focused sufficiently uniformly within one 10- μ m-square cross-section of one addressable volume element. Then the incident radiation density I_1 equals 5.18×10^{29} photons $\text{m}^{-2} \text{s}^{-1}$. To estimate N_S , we shall assume a 5 atomic percent doping of the original material with sensitizer molecules; of course this doping level cannot be too high or it is likely to interfere with the polymerization. If the sensitizer particles have a molecular weight of around 125, and the overall specific gravity is around 1, then $N_S \approx 2.4 \times 10^{26} \text{ m}^{-3}$. The decay time of S_1 will ordinarily be short compared to the cycle time; let us take $\tau_S = 1 \text{ ns}$. Then we find $G_S = 4.3 \times 10^{-5}$. Generally G_S will be much less than unity; this permits some simplifications in Eq. (17), but these are not worth discussing here except to note that as long as G_S is small, the exact value of τ_S is immaterial.

In favorable cases, the fractional transfer probabilities might be as high as 0.8, which value we shall adopt for both the S-to-T and the T-to-P transfer processes. For the singlet-state pumping time, 0.98 μ s turns out to be a satisfactory value, and with these parameters we find that after this time has elapsed

$$N_T / N_S = 0.0332, \quad (21)$$

or $N_T = 8.0 \times 10^{24}$ triplet-state molecules per m^3 when the triplet state pump is turned on. At this time, also, $N_S^*/N_S = 0.9668$; so clearly several pump cycles could be provided if necessary to overcome beam attenuation effects without seriously depleting the ground state.

For the triplet-state pump, we will assume a laser operating at 647.1 nm with a power of 2 W. This might be a krypton laser or a dye laser. An examination of available triplet absorption spectra indicates the absorption coefficient at this wavelength might be in the range 100 to 500 cm^{-1} . We have used the value 127 cm^{-1} , which gives $g_T = 0.50$ with the other parameters stated. Using such a value along with $f_T = 0.8$ and $\rho_T = 10$, corresponding to τ_T also equal to 1 ns, we find from Eq. (18) that $N_p \approx N_T$; that is, practically all the lowest-triplet-state molecules are transferred to the initiator state, so there are about 8.0×10^9 initiator molecules per beam-interaction spot 10 μ m on a side. If the remaining 95 atomic percent of the starting material is all monomer with a molecular weight of 100, there are about 5.7×10^{12} of these molecules per spot at the outset. Thus to polymerize the entire spot in one cycle, each initiator site will have to link up, on the average, some 720 monomer units. It should be clear from the discussion that the operating conditions could be varied quite substantially without markedly affecting this ratio.

With the high laser powers involved in the processes described here, it is natural to wonder about the temperature changes that might

result from the absorption of the beams. We can estimate upper limits for these effects in a very simple way by assuming that all the energy absorbed is converted to heat and that none of this energy is transported away from the beam interaction region. Then

$$I_{\text{abs}}\tau = C_m N_m \Delta T \quad , \quad (22)$$

where I_{abs} is the power absorbed from the pump beam in question within a suitable absorption volume, C_m is a suitably averaged molar heat capacity of the material, N_m is the number of moles affected, and ΔT is the temperature rise. For C_m we shall adopt a typical value of $20 \text{ J (mole K)}^{-1}$. To treat the singlet-state pump, let us assume that all 20 W are absorbed for $0.98 \mu\text{s}$ in the 10 cm long, $10 \mu\text{m}$ square rectangular parallelopiped in which we assume the laser beam intercepts the working volume. Then we find the average temperature rise in this region is around 1 K. Of course the calculated temperature rise near the entrance face will be somewhat greater. For the triplet-state pump, we have 2 W for $0.02 \mu\text{s}$ deposited in a cube $10 \mu\text{m}$ on a side; in this case the calculated temperature rise is about 19 K. Since we expect that only a relatively small portion of the absorbed energy will in fact be converted into heat, we conclude that heating effects are not likely seriously to interfere with system operation, at least when the operating conditions are normal.

There are a number of obvious ways that calculations of the type reported here could be modified and extended. At the present level of understanding, though, it is sufficient that they indicate a possibility that feasible operating conditions might conceivably be found; and more to the point than detailed numerical work is a conceptual study of ways the model we have developed indicates the system might fail to operate properly. We have just indicated, for instance, that heating effects of the laser beams can probably be dismissed. Another potential problem area that deserves attention is unwanted polymerization arising from the presence of residual lowest-triplet-state molecules in regions that we cannot

avoid intercepting with the triplet pump beam. The residual T_1 molecules may arise, of course, because of the slow decay of the triplet state. A number of systems approaches for mitigating or avoiding this problem immediately come to mind; and it should not be forgotten that a quantitative estimate to show that it really may be a problem has not yet been made; but we mention it as an example of the sort of considerations we plan to address in forthcoming work.

Design of New Photoinitiator Molecules

The research conducted during the past year has been focused on the design and development of new photoinitiator materials, as this is a crucial requirement for the successful operation of a PCM system. After considering a number of possible strategies for the design of a selective two-beam photoinitiator, the strategy shown schematically in Figure 3 was adopted as being the approach most likely to succeed. In this approach, as noted in the preceding section, a molecule is excited to its lowest excited singlet state (S_1) with photons from beam 1 having an energy below the dissociation threshold of the molecule and then rapidly undergoes intersystem crossing to its lowest triplet excited state (T_1). It is important that T_1 be transparent to light of the wavelength of beam 1, so no further excitation of the system can occur; in the absence of beam 2, therefore, the system will be inert, and T_1 will eventually decay harmlessly back to the ground state of the photoinitiator (S_0) with no chemical reaction taking place.

In the presence of beam 2, however, which is of a wavelength absorbed strongly by T_1 but not absorbed by the ground state, the photoinitiator will be excited to an upper triplet state, T_2 , with an energy content above the dissociation threshold for fragmentation of the molecule into reactive radicals (or ions). These species then initiate the actual polymer crosslinking process.

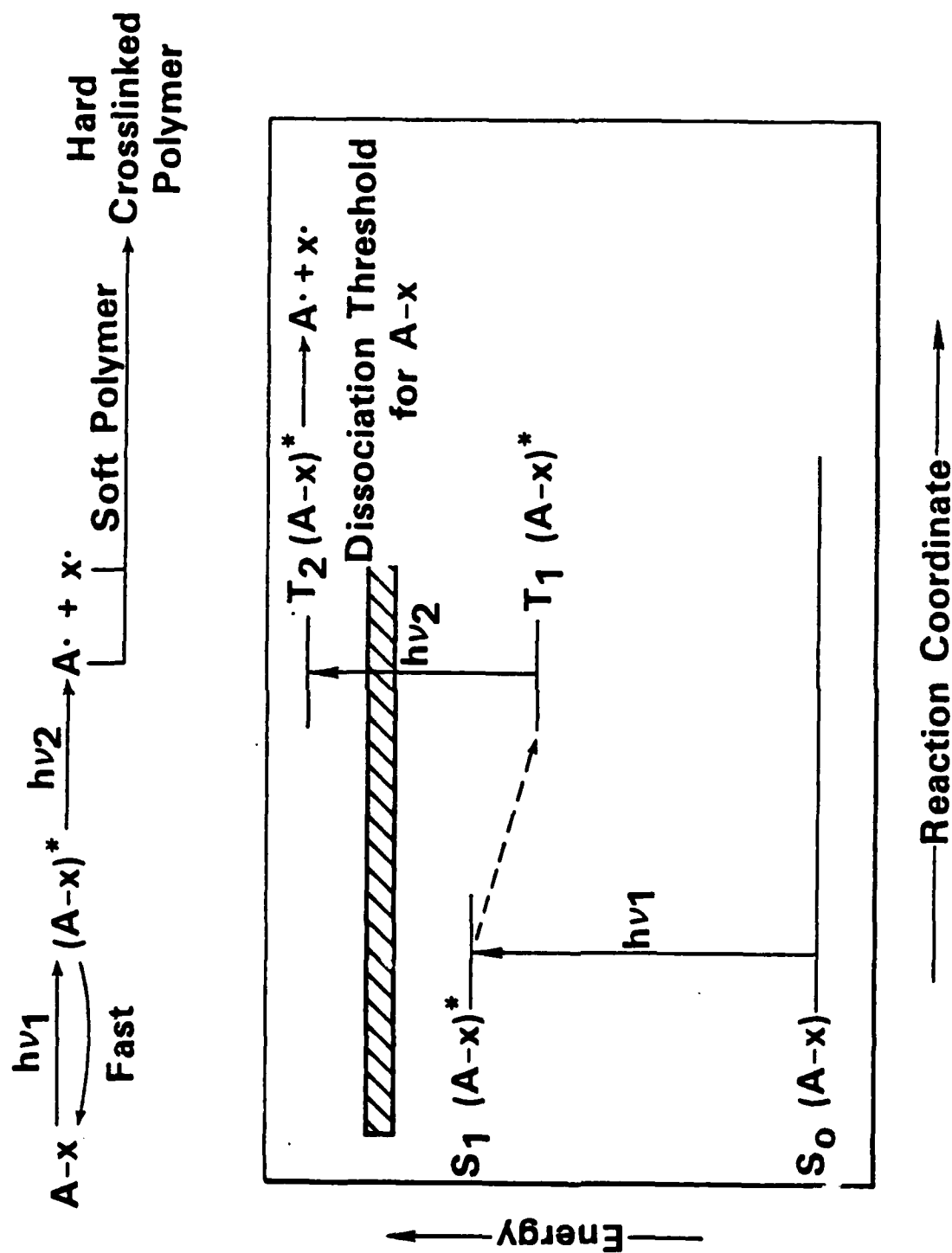
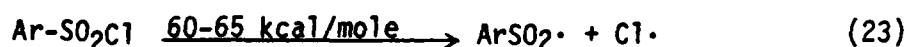


FIGURE 3. GENERAL STRATEGY FOR PHOTOINITIATOR DESIGN

The development of a successful photoinitiator molecule for PCM thus depends on the combination of two distinct functional groups: a light-absorbing moiety, or chromophore, with spectroscopic properties of the type just described, and a labile initiating group that can be fragmented with high efficiency once sufficient energy is contained in the molecule.

For this program, we have chosen to utilize two proven initiator groups for our candidate materials; these are the aryl sulfonyl chlorides and the benzylic bromides, as shown generically below. There is ample



precedent for the use of these initiating groups in commercial polymerization systems; both 2-naphthalene sulfonyl chloride and 2-bromomethylnaphthalene are in widespread use. The challenge, then, was to identify chromophoric groups (represented by "Ar" in the scheme above) which would exhibit the desired selectivity and still couple the energy of T_2 effectively into the initiator group.

As a starting point for this task, a compilation of spectroscopic data from the literature was prepared, so as to provide a facile means of comparing the properties of compounds for which triplet-triplet absorption spectra were known. These data are presented in Tables 1-3. While not exhaustive, they do provide valuable insights into the types of compounds that offer promise as chromophores for a PCM photoinitiator.

On the basis of these and other considerations (in particular, availability and/or ease of synthesis) three chromophores were chosen for initial study: these were 9,10-dibromoanthracene (an effective sensitizer from T_2 , its upper triplet state⁽²⁾); rubrene, or (5,6,11,12-tetraphenyl tetracene)⁽³⁾; and protoporphyrin IX dimethyl ester,⁽⁴⁾ which is representative of the porphyrin family of chromophores. The structures

TABLE 1. SUMMARY OF SPECTROSCOPIC DATA^(a)

Compound	E_s		E_{T_1}	E_{T_2}	$E_{T_1-T_2}$		ϵ_{T-T}	ϕ_{isc}
	(kcal/ mole)	(nm)	(kcal/ mole)	(kcal/ mole)	(kcal/ mole)	(nm)		
Azulene	40.6	704	30.9	--	--	--	--	--
Benzil	59.0	485	53.4	128.6 112.2	75.2 58.8	380.2 486.4	--	0.92
2,3-Butanedione (Biacetyl)	65.3	438	56.3	----See Table 2-----			--	1.00
Camphorquinone	~55	520	50	----See Table 2-----			--	1.00
Fluorenone	63.2	452	53.3	97.6	44.3	645.2	--	0.93
9,10-Dichloro- Anthracene	71.1	402	40.4	108.9	68.5	422.8	51,000	0.50
3,4-Benzopyrene	70.8	403	42.0	93.8	56.8	503.8	--	--
Pentaphene	67.5	423	48.4	--	--	--	--	--
Perylene	65.8	435	35.1	137.2 93.4	102.1 58.3	280 490	14,300	0.005
Tetralene	60.7	471	29.3	89.3	60.0	476.2	60,000	--

(a) From Reference 1, pp 316-327.

TABLE 2. TRIPLET-TRIPLET ABSORPTION SPECTRA OF CARBONYL COMPOUNDS^(a)

Compound	E_{T-T}			ϵ_{T-T}
	(kK)	(kcal/mole)	(nm)	
Benzaldehyde	32.50	92.92	307.69	(0.86)
	31.25	89.34	320.00	(1.00)
	27.40	78.34	364.96	(0.18)
	23.30	66.61	429.18	(0.11)
1-Naphthaldehyde	25.84	73.88	387.00	
	25.77	73.68	388.05	
	24.69	70.59	405.02	
	24.25	69.33	412.37	
	23.53	67.27	424.99	
	22.73	64.99	439.95	
	20.20	57.75	495.05	
Acetone	33.11	94.66	302.02	
Acetophenone	37.60	107.50	265.96	
	35.53	101.58	281.45	
Benzophenone	31.55	90.20	316.96	(1.00)
	23.98	68.56	417.01	(0.10)
	22.22	63.53	450.05	(0.14)
	20.20	57.75	495.05	(0.46)
	19.01	54.35	526.04	(0.68)
4-Aminobenzophenone	21.50	61.47	465.12	(1.00)
	15.62	44.66	640.20	(1.00)
3-Aminobenzophenone	21.99	62.87	454.75	(0.87)
	17.86	51.06	559.91	(1.00)
4-Hydroxybenzophenone	27.78	79.42	359.97	(1.00)
	19.42	55.52	514.93	(0.78)
Benzoin	27.03	77.28	369.96	(1.00)
	21.01	60.07	475.96	(0.95)
Fluorenone	30.50	87.20	327.87	(1.00)
	27.00	77.19	370.37	(0.36)
	25.80	73.76	387.60	(0.56)
	24.00	68.62	416.67	(0.82)
	23.20	66.33	431.03	(0.90)
	22.00	62.90	454.55	(0.70)
	18.10	51.75	552.49	(0.18)
	16.70	47.75	598.80	(0.22)
	15.50	44.31	645.16	(0.25)
	13.50	38.60	740.74	(0.10)
	11.00	31.45	909.09	(0.08)
2-Acetonaphthone	23.26	66.50	429.92	10,500
1-Acetylanthracene	22.90	65.47	436.68	(0.45)
	21.60	61.75	467.96	(0.70)
	21.00	60.04	476.19	(0.90)
	20.00	57.18	500.00	(1.00)
	18.20	52.03	549.45	(0.45)

TABLE 2. (Continued)

Compound	E_{T-T}			ϵ_{T-T}
	(kK)	(kcal/mole)	(nm)	
Biacetyl	45.45	129.94	220.02	5,160 in Benzene (RT)
	32.26	92.23	309.98	
	30.30	86.63	330.03	
	13.89	39.71	719.94	
	12.56	35.91	796.18	
	10.92	31.22	915.75	
	9.45	27.02	1058.20	
Camphorquinone	50.00	142.95	200.0	
	35.71	102.09	280.00	
	31.65	90.49	315.96	
	20.00	57.18	500.00	
	16.95	48.46	589.97	
	15.67	44.80	638.16	
	14.18	40.54	705.22	
	12.56	35.91	796.13	
	10.92	31.22	915.75	
	9.35	26.73	1069.52	
Benzil	26.30	75.19	380.23	
	20.56	58.78	486.38	
Acetylacetone	20.83	59.55	480.08	>>60
	19.23	54.98	520.02	
Trifluoroacetylacetone	26.32	75.25	379.94	>>30
	22.22	63.53	450.05	
Hexafluoroacetylacetone	25.64	73.30	390.02	1,000
	21.28	60.84	469.92	
3-Phenylacetylacetone	20.40	58.32	490.20	>3,000
Dibenzoylmethane	20.83	53.55	480.08	>1,500
	16.67	47.66	599.88	
	15.87	45.37	630.12	
	13.51	38.80	736.92	
Benzoylacetone	24.39	69.73	410.0	>1,500
	22.83	65.27	438.02	
	20.83	59.55	480.08	
	18.87	53.95	529.94	
	16.39	46.86	610.13	
Trifluorobenzoylacetone	17.24	49.29	580.05	18,000
	15.80	45.17	632.91	
Duroquinone	21.80(a)	62.33	458.72	5,330(b)
	20.40(a)	58.32	490.20	

(a) Liq Paraffin,
RT(b) Cyclohexane,
RT

TABLE 2. (Continued)

Compound	E_{T-T}			ϵ_{T-T}
	(kK)	(kcal/mole)	(nm)	
Anthraquinone	27.03	77.28	369.96	(1.00)
	24.69	70.59	405.02	(0.50)
	21.74	62.15	459.98	(0.28)
	19.05	54.46	524.93	(0.15)
	17.70	50.60	564.97	(0.12)
	16.26	46.49	615.01	(0.15)
	15.15	43.31	660.07	(0.16)
	14.81	42.34	675.22	(0.18)
Chloranil	20.83	59.55	480.08	
	20.00	57.18	500.00	
	18.52	52.95	539.96	
1,3,6',8'-Tetramethyl- Bianthrone	30.00	85.77	333.33	
	20.60	58.90	485.44	26,000
Benzoic Acid	31.25	89.34	320.00	
2-Aminobenzoic Acid	25.30	72.33	395.26	(0.90)
	23.00	65.76	434.78	(0.85)
	21.20	60.61	471.70	(1.00)
3-Aminobenzoic Acid	27.50	78.62	363.64	(0.85)
	24.30	69.47	411.52	(1.00)
3-Methylaminobenzoic Acid	27.50	78.62	363.64	(1.00)
	24.70	70.62	404.86	(0.55)
	23.00	65.76	434.78	(0.80)
3-Dimethylaminobenzoic Acid Methylester	28.00	80.05	357.14	(1.00)
	25.60	73.19	390.63	(0.30)
	24.30	69.47	411.52	(0.40)
	23.00	65.76	434.78	(0.40)
Benzamide	33.30	95.20	300.3	
	19.80	56.61	505.05	
2-Anthroic Acid	24.39	69.73	410.00	
	23.10	66.04	432.90	
Tetrachlorophthalic Anhydride	25.50	72.90	392.16	
	20.50	58.61	487.80	
	16.30	46.60	613.50	
Pyromellitic Dianhydride	25.70	73.48	389.11	
	20.20	57.75	495.05	
	18.50	52.89	540.54	

(a) From Reference 1, pp 326-327.

TABLE 3. TRIPLET-TRIPLET ABSORPTION SPECTRA OF ORGANIC DYESTUFFS^(a)

Compound	E_{T-T}			ϵ_{T-T}	
	(kK)	(kcal/mole)	(nm)		
Fluorescein	31.00a	89.75	318.57	4500a	(a) EtOH/Ether (90°K) (b) PMMA (77°K)
	27.00a	78.17	365.76	8000a	
	21.30a	61.66	463.65	9500a	
	19.60b	56.74	503.86	6000a	
	18.20b	52.69	542.62		
	15.75b	45.60	627.03	6500a	
	13.50b	39.08	731.53		
	12.65b	36.62	780.68		
	10.65b	30.83	927.29	4000a	
	9.20b	26.63	1073.44		
	8.75a	25.33	3267.43	13500a	
	6.00b	17.37	1645.94		
Dibromofluorescein	19.76	57.21	499.78	18000	
	30.80	89.17	320.64		
	23.20	67.16	425.67		
	21.80	63.11	453.01	28000	
	18.50	53.56	533.82		
	17.00	49.22	580.92		
Erythrosin	19.01	55.03	519.50	26000	
Proflavin	48.50	140.41	203.62	14000	
	47.50	137.51	207.91	12000	
	42.50	123.04	232.37	11500	
	38.00	110.01	259.89	SH	
	35.80	103.64	275.86	47000	
	28.50	82.51	346.51	6500	
	25.00	72.38	395.03	4000	
	18.20	52.69	542.62	12500	
	14.80	42.85	667.27	9000	
	10.65	30.83	927.29	13000	
	10.10	29.24	977.29	4000	
	9.10	26.34	1085.24	65000	
9-Phenylproflavin	48.50	138.7	206.2	30000	
	41.80	119.5	239.2	17500	
	35.50	101.5	281.7	47000	
	29.00	82.9	344.8	6000	
	26.00	74.3	384.6	8000	
	25.40	72.6	393.7	9000	
	17.40	49.7	574.7	12000	
	16.00	45.7	625.0	10000	
	14.50	41.5	689.7	11000	
	10.00	28.59	1000.0	8000	
	8.40	24.0	1190.5	40000	

TABLE 3. (Continued)

Compound	E_{T-T}			ϵ_{T-T}	
	(kK)	(kcal/mole)	(nm)		
Acridine Orange(a)	48.50	140.41	203.62	16000	(a) EtOH/Ether, 90°K
	41.00	118.70	240.87	17000	
	35.20	100.6	284.1	56000	
	28.50	81.5	350.9	5000	
	25.50	72.9	392.2	4000	
	18.60	53.2	537.6	10000	
	17.40	49.8	574.7		
	16.60	47.5	602.4	9500	
	15.50	44.3	645.2	10000	
	14.60	41.7	684.9		
	13.60	38.9	735.3		
	12.80	36.6	781.3		
	12.30	35.2	813		
	11.20	32.0	892.9		
	10.80	30.9	925.9	2500	
	9.60	27.4	1041.7		
	9.20	26.3	1087		
	8.60	24.6	1162.8	15500	
	8.10	23.2	1234.6	SH	
	7.90	22.6	1265.8	54000	
Acridine Yellow	16.50	47.2	606.0	(0.20)	
	10.00	28.59	1000.0	(1.00)	
Trypaflavin(b)	19.80	56.6	505		(b) PMMA, 77°K
	18.90	54.0	529	(0.32)	
	18.00	51.5	555.6		
	15.40	44.0	649.4	(0.29)	
	12.50	35.7	800.0		
	10.65	30.4	938.9		
	8.27	26.5	1078.7		
	8.40	24.0	1190.5	(1.00)	
Benzoflavin	7.70	22.0	1298.7		
	6.07	17.35	1647.4		
	13.35	38.2	749		
	10.50	30.0	952.4		
	9.10	26.0	1098.9		
	8.34	23.8	1199		
Thionine (pH=1)	7.70	22.0	1298.7		
	6.07	17.35	1647.4		
Thionine (pH=1)	26.70	76.3	374.5	14000	
	15.30	43.7	653.6	15500	
Thionine (pH=8)	24.10	68.9	414.9	11500	
	15.60	44.6	641.0	6300	
	13.10	37.5	763.4	9200	

TABLE 3. (Continued)

Compound	E_{T-T}			ϵ_{T-T}
	(kK)	(kcal/mole)	(nm)	
Auramine	14.30	40.9	699.3	
	9.20	26.3	1086.9	
	8.35	23.9	1197.6	
	7.70	22.0	1298.7	
Methyl Violet	18.50	52.9	540.5	
	15.90	45.5	628.9	
	8.10	23.2	1234.6	
Ethyl Violet	19.00	54.3	526.3	
	16.10	46.0	621.1	
	8.90	25.4	1123.6	
Crystal Violet	18.60	53.2	537.6	
	16.00	45.7	625	
	9.00	25.7	1111.1	
	8.00	22.9	1250.0	
Malachite Green	12.80	36.6	781.3	
Methylene Blue (pH=2)	26.70	76.3	374.5	
	23.80	68.0	420.2	
	21.30	60.9	469.5	
Methylene Blue (pH=7)	35.46	101.5	281.7	
	23.80	68.0	420.2	
	19.23	54.9	520.0	
	14.39	41.1	694.9	
	13.70	39.2	729.9	
	13.07	37.4	765.1	
	12.66	36.2	789.9	
	11.56	33.1	865.1	
Methylene Green	24.40	69.8	409.8	
	19.25	55.0	519.5	
	13.15	37.6	760.5	
	12.65	36.2	790.5	
Novomethylene Blue	23.80	68.0	420.2	
	12.80	36.6	781.2	
Safranine T (pH=9)	26.30	75.2	380.2	
	13.30	38.0	751.9	
Safranine T (pH=5)	25.60	73.2	390.6	
	15.40	44.0	649.4	
	13.90	39.7	719.4	
Phenosafranine (pH=9)	26.00	74.3	384.6	
	13.70	39.2	729.9	

TABLE 3. (Continued)

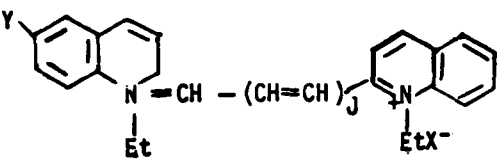
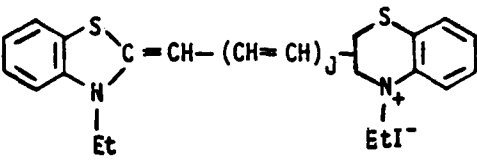
Compound	E_{T-T}			ϵ_{T-T}
	(kK)	(kcal/mole)	(nm)	
Phenosafranine (pH=5)	25.30 16.25 15.05	72.3 46.5 43.0	395.3 615.4 664.5	
Rhodamine B	16.00	45.7	625	13500
<u>Cyanine Dyes:</u>				
				
J=0, X=I, Y=H	15.80	45.2	632.9	
J=0, X=I, Y=Br	15.40	44.0	649.3	
	20.00	57.2	500.0	
J=0, X=I, Y=I	15.00	42.9	666.7	
	14.90	42.6	671.1	
J=1, X=Cl, Y=H	13.50	38.6	740.7	
<u>Thiacyanine Dyes:</u>				
				
J=0	17.70 16.00 15.00 14.10	50.6 45.7 42.9 40.3	564.9 625 666.7 709.2	(0.16) (1.00) (0.85) (0.85)
J=1	11.50 11.00 10.75	32.9 31.4 30.7	869.6 909 930	(0.53) (0.88) (1.00)
J=2	10.20 9.85	29.2 28.2	980.4 1015.2	(0.45) (1.00)
<u>Biological Interest Compounds:</u>				
Thymine	30.09	85.99	332.4	
Orotic Acid	27.40 23.20	78.34 66.3	364.9 431.0	
All trans- β -Carotene	22.20 20.80 19.60	63.47 59.47 56.0	450.5 480.8 510.20	66500 107000 130000

TABLE 3. (Continued)

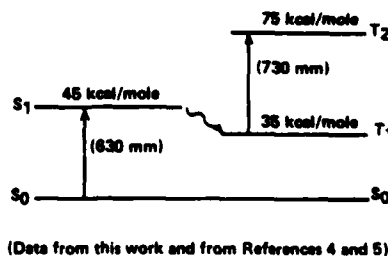
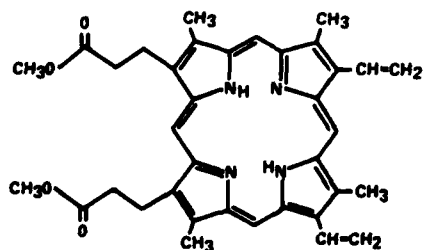
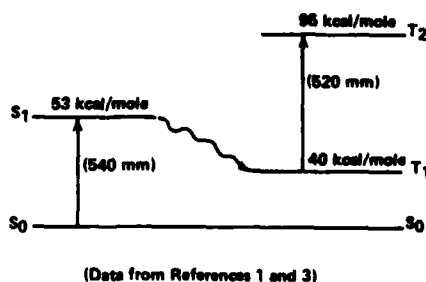
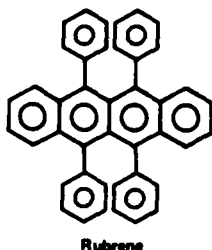
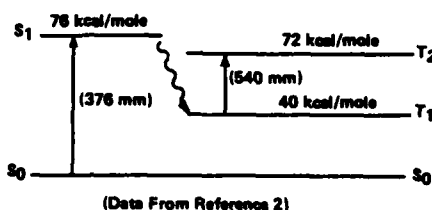
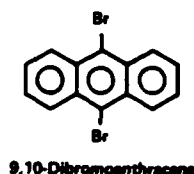
Compound	E_{T-T}			ϵ_{T-T}
	(kK)	(kcal/mole)	(nm)	
<u>Biological Interest Compounds (Cont.)</u>				
All <u>trans</u> -Lycopene	21.90	62.61	456.62	39000
	20.50	58.61	487.80	152000
	19.25	55.04	519.48	390000
	19.00	54.32	526.32	258000
	18.00	51.46	555.56	78000
<u>Cis/trans</u> -Lycopene	19.20	54.89	520.83	
Retinene	22.22	63.53	450.05	75800
Pheophytin-a	30.00	85.77	333.33	50000
	24.50	70.05	408.16	63000
	19.00	54.32	526.32	17800
	14.80	42.31	675.68	4700
Pheophytin-b	23.80	68.04	420.17	71000
	21.00	60.04	476.19	31500
	15.30	43.74	653.59	5700
Chlorophyll-a	21.70	62.04	460.83	32000
	18.90	54.04	529.10	17800
	16.40	46.89	609.76	
	15.20	43.46	657.89	
Chlorophyll-b	26.30	75.19	380.23	19700
	22.50	64.33	444.44	26000
	20.65	59.04	484.26	34700
	18.20	52.03	549.45	21500
	16.55	47.32	604.23	12000
	15.50	44.31	645.16	
Zr-Chlorophyll-a	22.20	63.47	450.45	
Chlorophylline	21.30	60.90	469.48	
	19.22	54.95	520.29	
Bacteriochlorophyll	24.40	69.76	409.84	22200
	20.00	57.18	500.00	10000
	16.15	46.17	619.20	11500
	15.25	43.60	655.74	9300
Methylchlorophyllide	21.30	60.90	469.48	
	19.22	54.95	520.29	
Pheophorbide	20.85	59.61	479.62	
	17.25	49.32	579.71	

TABLE 3. (Continued)

Compound	E_{T-T}			ϵ_{T-T}
	(kK)	(kcal/mo ¹ e)	(nm)	
<u>Biological Interest Compounds (Cont.)</u>				
Tetraphenylporphin	29.00	82.91	344.83	33000
	25.65	73.33	389.86	42000
	23.25	66.47	430.11	83000
	14.50	41.46	689.66	3500
	12.80	36.60	781.25	6000
Zn-Tetraphenylporphin	25.00	71.48	400.00	42000
	21.30	60.90	469.48	74000
	13.42	38.37	745.16	5300
	11.85	33.88	843.88	8200
Photoporphyrin	28.60	81.77	349.65	(0.90)
	23.80	68.04	420.17	(1.00)
	(19.80)	56.61	505.05	(0.22)
	(18.90)	54.04	529.10	(0.15)
	(17.25)	49.32	579.71	(0.06)
	(15.90)	45.46	628.93	(0.08)
Zn-Protoporphyrin	22.00	62.90	454.55	(1.00)
	(18.55)	53.03	539.08	(0.13)
	(17.10)	48.89	584.80	(0.09)
	(15.65)	44.74	638.98	(0.08)
Mesoporphyrin	22.20	63.47	450.45	
Tetraphenylchlorin	21.30	60.90	469.48	
	(19.25)	55.04	519.48	
Coproporphyrin	27.80	79.48	359.71	(0.75)
Dimethyl Ester	25.60	73.19	390.63	(1.00)
	23.60	67.47	423.73	(0.90)
	20.00	57.18	500.00	(0.27)
Mg-Phthalocyanine	25.00	71.48	400.00	(1.00)
	21.30	60.90	469.48	(0.78)
Rubrene	23.90	68.33	418.41	(0.25)
	19.25	55.04	519.48	(1.00)
	18.60	53.18	537.63	(0.58)

(a) From Reference 1, p 335.

and approximate energy levels of these systems are shown below. The bulk of the experimental work during this first year's effort has focused on the dibromoanthracene system, because of its attractive spectroscopic properties and its widespread commercial availability. Much of our work since then has been directed toward the synthesis of modified chromophores containing the desired initiating groups, and evaluating the behavior of these photoinitiators in various monomers and polymers, particularly methyl methacrylate. Dibromoanthracene (Aldrich) was used as is, after purification by recrystallization from ethanol. Rubrene and protoporphyrin IX

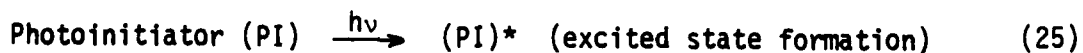


dimethylester were brominated according to standard procedures, although the expected "rubrene dibromide" described in the literature⁽⁶⁾ was not obtained under our conditions; rather, a polybrominated rubrene derivative of unknown structure was obtained. Methyl methacrylate was distilled from molecular series under argon and stored over molecular sieves under argon in a freezer at around -10 C. Other procedural details are reported in the context of the experiments described below.

Photoinduced Crosslinking of Polymers

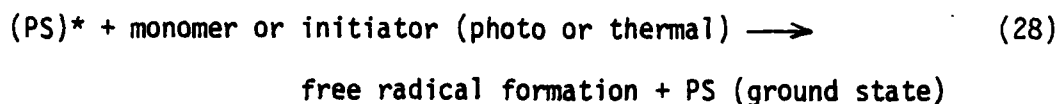
The photopolymerization of a vinyl monomer/polymer system is best effected through the use of special photoactive catalyst molecules. These photoactive catalyst molecules must be capable of absorbing light energy and be able to undergo efficient photochemical transformation or interaction to produce vinyl monomer/polymer-initiating free radical intermediates⁽⁷⁻¹⁴⁾. The nomenclature associated with chemical structures of organic, organometallic or inorganic compounds and their ability to produce free radical intermediates upon light absorption is presently somewhat confusing.^(15,16)

A photoinitiator in this discussion represents a molecule which, upon absorption of light energy of appropriate wavelength and intensity, undergoes photophysical transformation to its excited states, having total energy content in excess of that required to effect bond rupture (homolytic scission) in the molecule and subsequent formation of free radical intermediates.



A photosensitizer can be a compound which upon absorption of light energy undergoes photophysical transformation to its excited states

followed by inter- or intramolecular energy transfer to another compound, monomer or initiator (photo or thermal) which then results in the production of free radical intermediates.



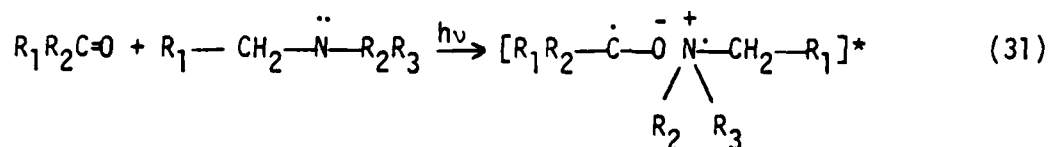
The basic difference between both free radical intermediate generating systems is that, in one case, the photoinitiator is physically changed or destroyed while, in the other case, the photosensitizer is not consumed but acts only as an energy transfer agent.(15-18)

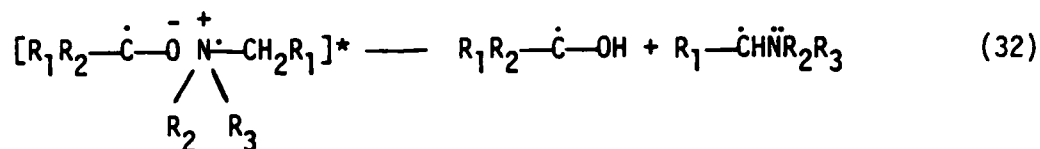
Photoreduction is another method by which a photosensitizer can produce active free radical intermediates. In this type of reaction an excited state photosensitizer molecule interacts with a ground state substrate containing an active hydrogen atom. The net result is that the photosensitizer becomes partially reduced to form a free radical intermediate and the substrate containing the donor hydrogen atom is also transformed into a free radical intermediate species.(19,20)



(hydrogen donor compound)

Another important process, in which a photosensitizer (specifically, aromatic carbonyl derivatives) can undergo electron-transfer complex formation resulting in photoreduction and subsequent formation of free radical intermediates, is as follows:





Each of the mechanisms for free radical intermediate production (photoinitiation, energy transfer, photoreduction, electron-transfer complex formation) will be discussed in the following sections.

Light Absorption. The first step in any photochemical reaction is the absorption of light energy, emitted from a given source, by the reacting molecule (in this case the photoinitiators or photosensitizers are the absorbing species). Since the light absorption process of a molecule is fundamental to photochemical reaction efficiency it is important to select photoinitiator and photosensitizer chemical structures that have light energy absorption bands which overlap the emission spectra of the light source used in the photochemical process. The probability of light absorption by a molecule is governed by the arrangement of atoms in the molecule and their surrounding environments.(21-24)

The basic UV and visible absorption spectra of aromatic ketones and mixed aromatic-aliphatic ketone structures associated with photoinitiator or photosensitizer compounds involves electronic transition between π (bonding) and π^* (antibonding) molecular orbitals characteristic of aromatic molecules as well as n (non-bonding) to π^* transitions associated with various carbonyl compounds.(25-28) The probability of absorption is measured or related to an experimental absorption coefficient or extinction coefficient (ϵ). By definition here, ϵ refers to the molar decadic (base 10) extinction coefficient; ϵ has units of $\text{l mol}^{-1} \text{cm}^{-1}$. Aromatic structures undergoing $\pi-\pi^*$ transitions usually have large values for ϵ , while $n-\pi^*$ transitions are usually forbidden because of symmetry but are observable through vibronic coupling; they have relatively low values for ϵ .(25-29)

A list of typical photoactive parent organic molecules, photo-initiators, photosensitizers and their extinction coefficients is given in Table 4. In Fig. 4 is shown an extinction coefficient versus absorption wavelength of light energy representation for a series of aromatic ketone photosensitizers.(30-31)

TABLE 4. MOLECULAR STRUCTURE-EXTINCTION COEFFICIENT RELATIONSHIPS^(a)

Molecule	Extinction Coefficient, E		
Photosensitive Parent Molecule	$\lambda = 254 \text{ nm}$	$\lambda = 313 \text{ nm}$	$\lambda = 366 \text{ nm}$
Acetone	7	3	0
Acetophenone	10^3	4×10^1	5
Benzophenone	1.7×10^4	5×10^1	7×10^1
4,4'-Bis(N,N-dimethyl amino)benzophenone	1.3×10^4	1.1×10^4	2.8×10^4
Benzene	9×10^1	0	0
Toluene	1.7×10^2	0	0
Xanthone	1×10^4	3×10^3	2×10^2
Photosensitizer	$\lambda = 318-320 \text{ nm}$	$\lambda = 340-345 \text{ nm}$	
Benzoin	310	--	
α -Methylbenzoin	200	--	
α -Hydroxymethyl benzoin	--	150	
Benzoin isopropyl ether	--	230	
Benzoin phenyl ether	--	250	

(a) From: V. D. McGinniss, in "Developments in Polymer Photochemistry - 3", N. S. Allen, Ed., Applied Science Publishers, Ltd., Essex, England (1981), Chapter 1.

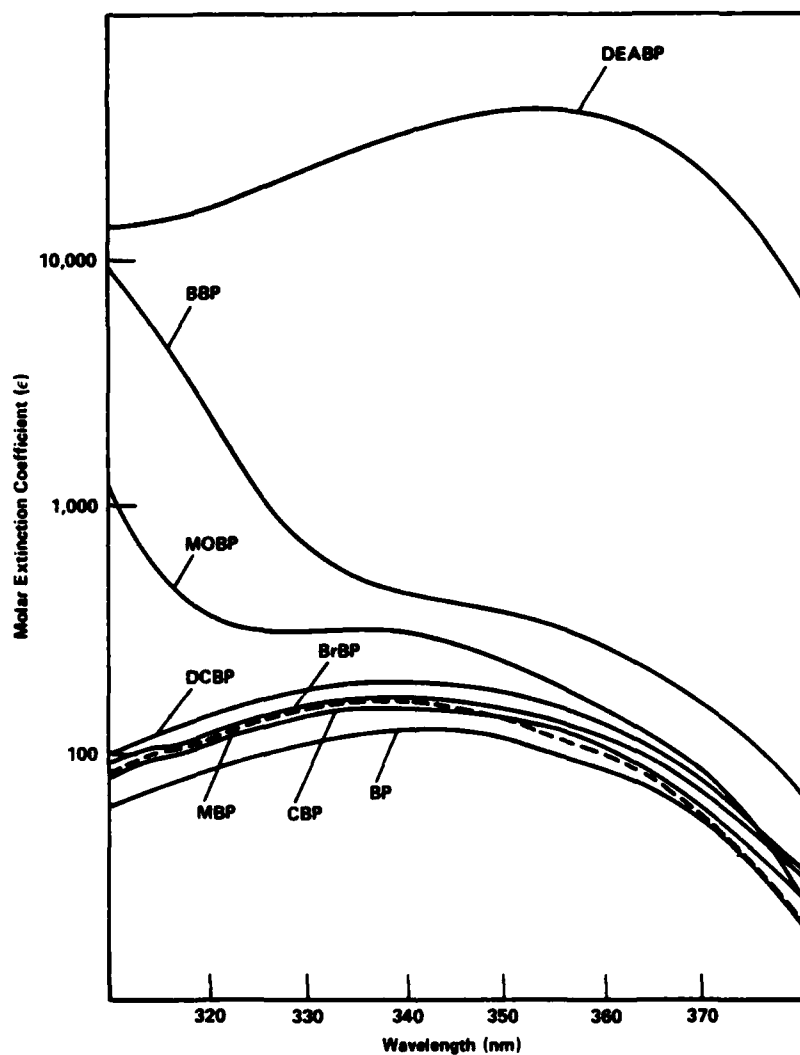


FIGURE 4. EXTINCTION COEFFICIENT (ϵ) AND λ_{\max} VALUES FOR THE FOLLOWING SERIES OF p-SUBSTITUTED BENZOPHENONE DERIVATIVES: BENZOPHENONE (BP), BISDIETHYLAMINOBENZOPHENONE (DEABP), BENZOYL BENZOPHENONE (BBP), METHOXYBENZOPHENONE (MOBP), DICHLOROBENZOPHENONE (DCBP), BROMOBENZOPHENONE (BrBP), METHYLBENZOPHENONE (MBP) AND CHLOROBENZOPHENONE (CBP).

Photophysical Processes

After absorption of light energy, followed by changes in electron distribution, the excited molecules can undergo various types of photophysical or photochemical deactivation pathways (Fig. 5).

Most organic molecules have paired electrons in their ground state (S_0) and upon absorption of light energy a change in electron distribution takes place in which electrons are promoted to upper singlet

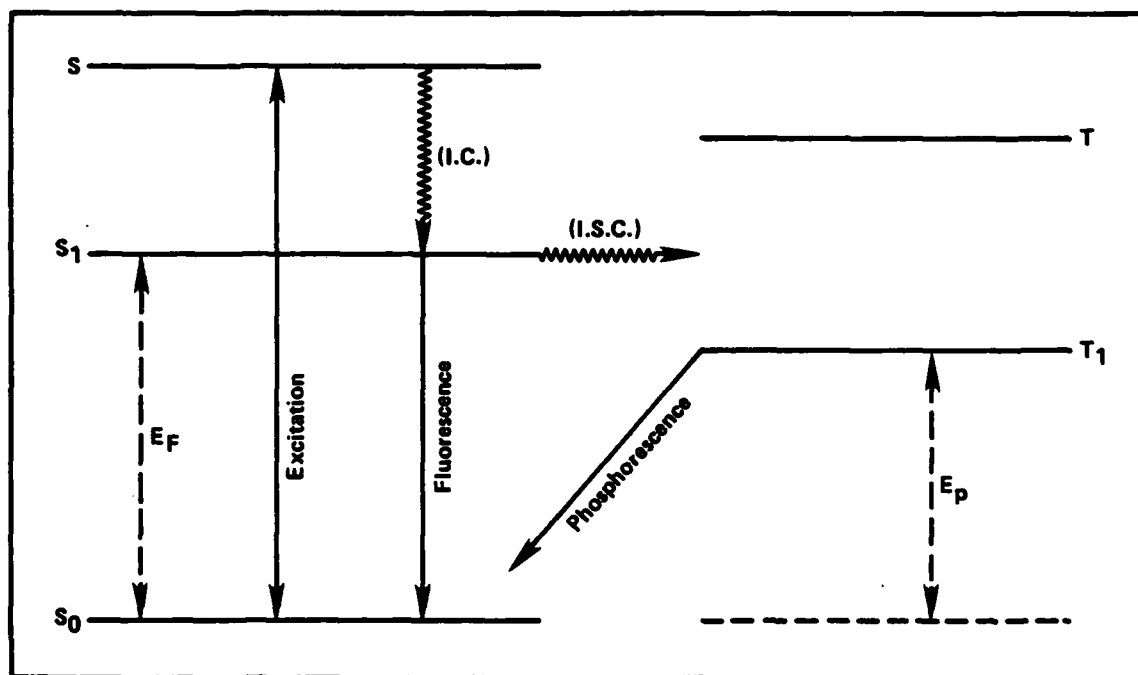


FIGURE 5. JABLONSKI DIAGRAM. S_0 = GROUND STATE; S = UPPER SINGLET LEVEL; S_1 = LOWEST SINGLET LEVEL; E_F = ENERGY OF LOWER SINGLET STATE; T_1 = LOWEST TRIPLET LEVEL; T = UPPER TRIPLET LEVEL; E_p = ENERGY OF LOWEST TRIPLET STATE; I.C. = RADIATIONLESS INTERNAL CONVERSION PROCESS; I.S.C. = RADIATIONLESS INTERSYSTEM CROSSING PROCESS

level (S_1 , S_2) excited states with conservation of their electron spin configurations. Loss of this absorbed energy without molecular rearrangement can result from internal conversion or through fluorescence radiative processes.

A second process, especially important to aliphatic or aromatic carbonyl compounds, is the ability of an excited state molecule (S_1 , S_2 energy levels) to undergo a change in electron spin configuration through intersystem crossing a lower triplet energy level excited state. Emission of light energy from the triplet level results in phosphorescence radiative processes.

Another factor to consider is the efficiency with which the incident radiation on the absorbing molecules is converted to the triplet excited state. This efficiency can be defined in the following manner:

$$\begin{aligned} \phi_p \text{ (quantum yield of phosphorescence)} \\ = \frac{\text{number of triplet states which emit light}}{\text{number of photons absorbed by the molecules}} \end{aligned} \quad (33)$$

Photoinitiators or photosensitizers having chemical structures that facilitate intersystem crossing processes and enhance ϕ_p would be expected to exhibit efficient free-radical-intermediate generating capabilities(26,29,32)

The energy and reactivity of the triplet states of a photoinitiator or photosensitizer are also important considerations, since most excited state photochemical reactions (molecular rearrangement, free radical intermediate formation and hydrogen abstraction reactions) occur from the triplet energy levels of these types of chemical structures. If the triplet lifetime of the photoinitiator or photosensitizer is short, then the chance of reaction, formation of free radical intermediates or undergoing hydrogen abstraction processes is less than if the triplet lifetime were long. If the triplet energy levels for photoinitiators or photosen-

sitizers are low, it is possible that other chemical molecules in the photoreactive system (oxygen or certain monomer chemical structures) will cause quenching of the triplet excited state which subsequently lowers the ability of a photoinitiator or photosensitizer to effect free radical generation processes.(12,33) Examples of typical triplet lifetimes and triplet energies for aromatic and aromatic-aliphatic carbonyl compounds are listed in Table 5.(30)

TABLE 5. MOLECULAR STRUCTURE-TRIPLET ENERGY RELATIONSHIPS

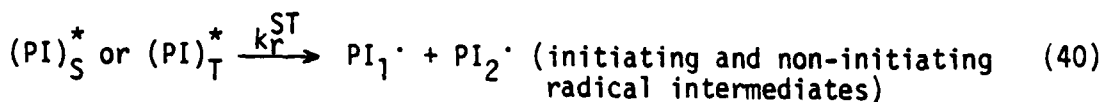
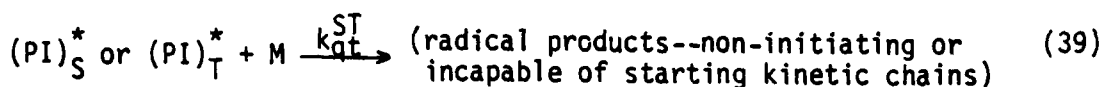
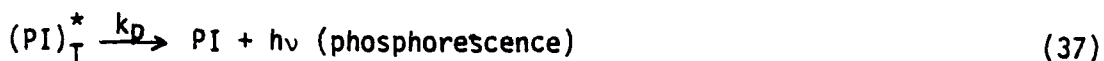
Photosensitive Parent Molecule	Triplet Energy (kcal/mol)	Triplet Lifetime in Solution (μ s)
Acetone	79-82	0.94
Acetophenone	73-4	3.50
Benzophenone	68-9	12.0
4,4'-Bis(N,N-dimethyl-amino)benzophenone	62	27
Xanthone	74	50

Mechanisms For Photochemical Production of Free Radical Intermediates

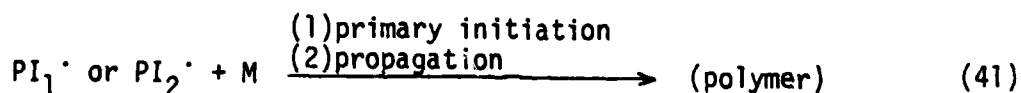
In order to describe the mechanism of a photochemical reaction it is necessary to evaluate and quantify the following processes:

1. light absorption;
2. radiative decay (fluorescence);
3. intersystem crossing efficiency;
4. phosphorescence;
5. molecular rearrangement; and
6. quenching.

For photoinitiators (PI) the primary photochemical reactions are as follows



The optimum efficiency of photoinitiation is achieved if all fragment radical intermediates (PI_1 and PI_2) react rapidly with a monomer (M) and start the growth of kinetic chains (primary initiation).



Another expression representing radical formation efficiency can be defined in the following manner:

$$\text{Rate of radical production} = \alpha_{PI} = (PI)_S^* k_r^{ST} \quad (42)$$

If we assume $(PI)_T$ is more important than $(PI)_S$ for the formation of radical intermediates then

$$\alpha_{PI} = (PI)_T^* k_r^T \quad (43)$$

The rationale for this expression is that most photoinitiator molecules are composed of aromatic carbonyl chemical structures having long-lived triplet excited states, high k_{ST} values and low k_f efficiencies, hence

$$d(PI)_T^*/dt = (PI)_S^* k_{ST} - (PI)_T^* k_p - (PI)_T^* [M] k_{qn}^T - (PI)_T^* [M] k_{qr}^T - (PI)_T^* k_r^T \quad (44)$$

Invoking steady state kinetic analysis conditions for $(PI)_S$ and $(PI)_T$ leads to

$$(PI)_S^* = \frac{[PI] I_0 \epsilon}{k_f + k_{ST} + [M] k_{qn}^S + [M] k_{qr}^S + k_r^S} \quad (45)$$

$$(PI)_T^* = \frac{(PS)_S^*}{k_p + [M] k_{qn}^T + [M] k_{qr}^T + k_r^T} \quad (46)$$

If we assume $k_{ST} \approx 1$, $k_f = 0$ and

$$k_{qn}^S = k_{qr}^S = k_r^S \ll k_{qn}^T = k_{qr}^T = k_q \quad (47)$$

then

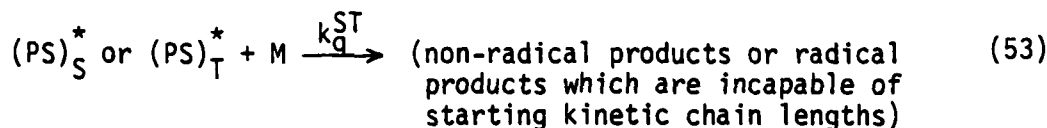
$$(PI)_T^* = \frac{[PI] I_0 \epsilon}{k_p + [m] k_q + k_r^T}$$

Substitution of eqn (47) into eqn (43) results in (48)

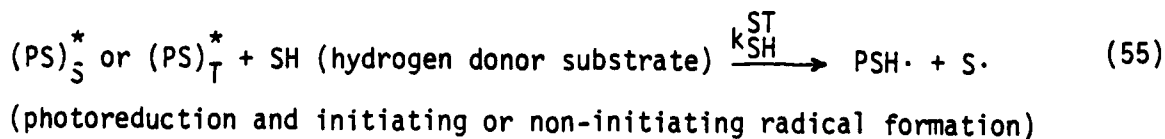
$$\alpha_{PI} \text{ (rate of radical production)} = \frac{[PI] I_0 \epsilon k_r^T}{k_p + [M] k_q + k_r^T}$$

If the rate constants for phosphorescence (k_p) and quenching (k_q) are larger than the radical formation rate constant (k_r^T) then the rate of radical production (α_{PI}) will be very small and inefficient. It is desirable to design photoinitiator molecules whose chemical structures enhance the t_r rate constant over the deactivation pathways. (34-37)

A similar reaction scheme can also be derived for photosensitizers (PS):



$I \cdot$ (free radical formation) + PS



If we assume similar arguments apply as derived for photoinitiators then

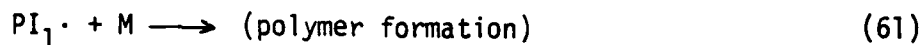
$$\alpha_{PS} \text{ (rate of free radical production)} = (PS)_T^* [I] k_I^T \quad (56)$$

$$\alpha_{PS} \text{ (rate of free radical production)} = (PS)_T^* [SH] k_{SH}^T \quad (57)$$

$$\alpha_{PS} = \frac{[PS] I_0 \epsilon [I] k_I^T}{k_p + k_q [M] + [I] k_I^T} \quad (58)$$

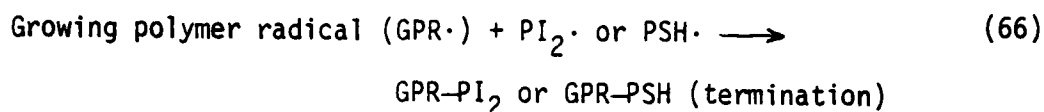
$$\alpha_{PS} = \frac{[PS] I_0 \epsilon [SH] k_{SH}^T}{k_p + k_q [M] + [SH] k_{SH}^T} \quad (59)$$

It should be noted that not all free radical intermediates produced through photochemical reactions are primary initiators, in that certain structures may be incapable of starting kinetic chain growth of a vinyl monomer:



It should also be noted that solvent factors and the actual chemical structure of the vinyl monomer (M) may ultimately determine whether or not a primary radical intermediate undergoes initiation or termination kinetic processes.

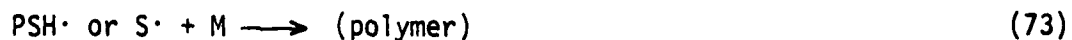
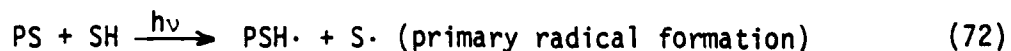
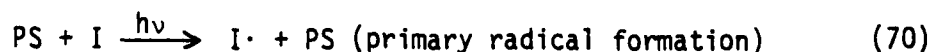
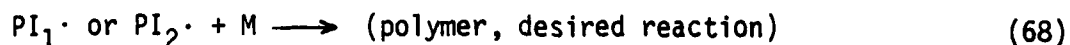
In some cases a certain free radical intermediate chemical structure may only participate in termination reactions with a growing polymer chain. (12,30,38,39)



All of the above factors must be considered when designing and selecting photoinitiators or photosensitizers for use in photopolymerization reactions.

Photopolymerization

The function of a photoinitiator or photosensitizer molecule is to provide primary initiating free radical intermediates in a photopolymerization reaction system. The greater the efficiency for primary radical production as well as the minimum competitive interactions between primary radicals and vinyl monomer determines the overall rate of photopolymerization.



For the following discussion $PI_1\cdot$, $PI_2\cdot$, $I\cdot$, $PSH\cdot$ and $S\cdot$ will be designated as primary radicals ($PR\cdot$).

The overall rate of a photopolymerization reaction can be expressed as a function of initiation of the chain radicals, propagation of chains and termination processes. The rate of initiation (R_i) can be described in the following manner:

$$\begin{aligned}
 R_i = & \text{(primary radical formation)} \\
 & - \text{(primary radical interaction with vinyl monomers)} \\
 & - \text{(primary radical competitive interactions leading to} \\
 & \quad \text{non-polymeric products)}
 \end{aligned}
 \tag{75}$$

Primary radical ($PR\cdot$) formation is given by

$$(PR\cdot) = I_0 \phi l \epsilon [PI \text{ or } PS] \tag{76}$$

where I_0 = incident light intensity, ϕ = quantum yield for radical production ($\phi = 2$ when 1 quantum absorbed results in 2 primary radicals having equal activity and $\phi < 2$ is due to competitive processes), l = optical path length of the system ϕ and ϵ = photoinitiator (PI) or photosensitizer (PS) molar extinction coefficient.

Now,

$$\text{primary radical initiation} = k_1 [PR\cdot][M] \tag{77}$$

and,

$$\text{primary radical competitive processes} = k_{cp} 2[PR\cdot]^2 \tag{78}$$

If we assume that in many cases primary radical competing processes are at a minimum then

$$\text{rate of initiation } (R_i) = I_0 \phi l \epsilon [PI \text{ or } PS] = k_1 [PR\cdot][M] \tag{79}$$

The overall rate of a photopolymerization reaction (R_p) can be described by the following equation:

$$R_p = \frac{d[M]}{dt} = \frac{k_p[M]R_i^{1/2}}{k_t^{1/2}} \quad (80)$$

where k_t = termination rate constant (liter/mols), k_p = propagation rate constant (liter/mols), $[M]$ = monomer concentration (mol/liter), and R_i = rate of initiation (mol/liters).

If the rate constants for k_r , k_p , k_q , k_I , k_{SH} are known then values α_{PI} and α_{PS} (eqns (48) (58) and (59)) can be calculated. Also, according to Eqn (80) the rate of photopolymerization (R_p) should be proportional to $\alpha_{PI}^{1/2}$ or $\alpha_{PS}^{1/2}$ if one assumes R_i to be proportional to α_{PI} or α_{PS} .

The quantum yield for the number of kinetic chains started per photon absorbed by the photoinitiator or photosensitizer is defined as follows:

$$\phi_i = f_p \phi(\alpha_{PI} \text{ or } \alpha_{PS}) \phi(\text{triplet}) \quad (81)$$

where f_p = fraction of radicals starting kinetic chains, ϕ = quantum yield for number of primary radicals formed (in α -cleavage reactions, $\phi = 2$) and $\phi(\text{triplet})$ = quantum yield of triplet formation.

The use of photochemical and photopolymerization reaction kinetic analysis techniques helps one to better understand fundamental concepts associated with various chemical structures for photoinitiator and photosensitizer systems. (34-37,40)

Polymeric Crosslinking Reactions

In conventional monofunctional vinyl unsaturated monomer polymerization reactions, the liquid monomer undergoes an initially slow reaction sequence to form a solid mass of material (Figure 6). About half way through the reaction sequence the monomer/polymer ratio reaches a critical value (gel point) and a rapid rise in solution viscosity is noticed along with an autoacceleration in the rate of polymerization reaction. The final stages of conversion are relatively slow in that the monomer/polymer ratio is very low and the low molecular weight monomer units must diffuse into large macroradical structures in order to terminate the polymerization process.

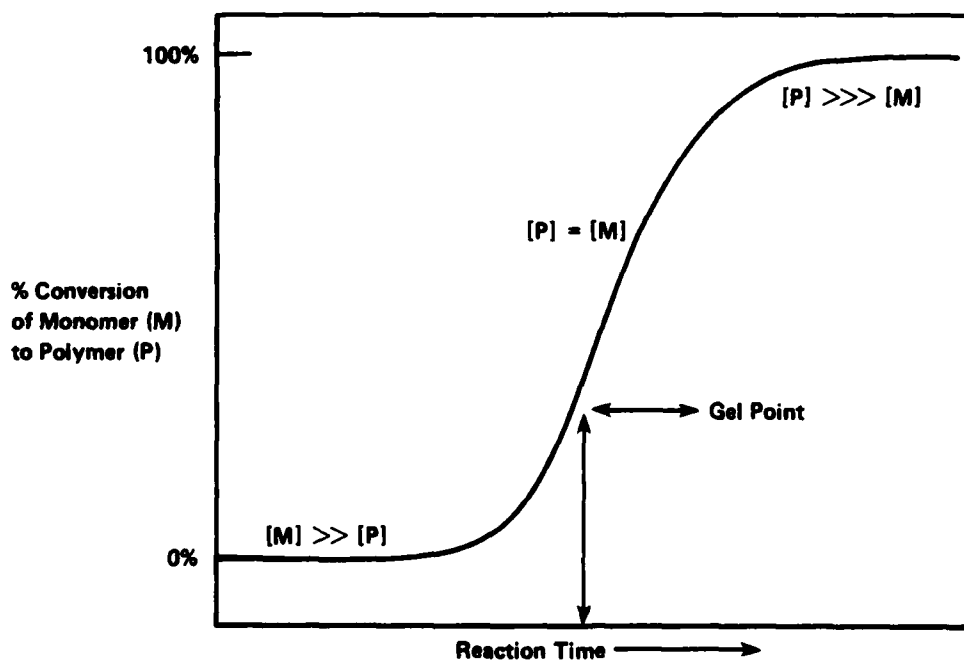


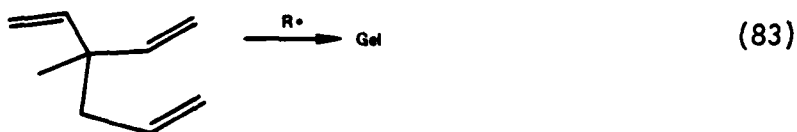
FIGURE 6. TIME SEQUENCE OF A TYPICAL VINYL POLYMERIZATION REACTION

Analysis of the overall rate equation for photoinduced polymerization reactions,

$$R_p = \frac{K [\text{monomer}][\text{photoinitiator}]^{1/2}}{k_t^{1/2}} \quad (82)$$

indicates that any substantial change in k_t (termination rate constant) strongly influences the rate of reaction. Since k_t has an indirect relationship to the monomer/polymer solution viscosity [$k_t = f(1/\eta)$ and $\eta = f(\text{monomer/polymer})$] then the % conversion of monomer to polymer can be accelerated under certain conditions directly related to monomer or polymer concentration effects.

The most efficient method of converting a liquid reactive monomer system to a solid polymer is through the use of multi functional vinyl unsaturated monomers that are capable of quickly developing gel or network structures at very low percentages of conversion.



The photoinduced addition polymerization of multifunctional monomers proceeds in general in three stages: formation of linear ("primary") macromolecules with pendent functional groups, branching through these groups and, finally, intermolecular crosslinking leading to gelation, i.e., the occurrence of macromolecules of "infinite" molar mass.⁽⁴¹⁾ In addition, intramolecular cyclization reactions may occur which, in special cases, lead to cyclopolymerizations and the absence of gelation.⁽⁴²⁾ Differences of opinion exist as to the relative extent of

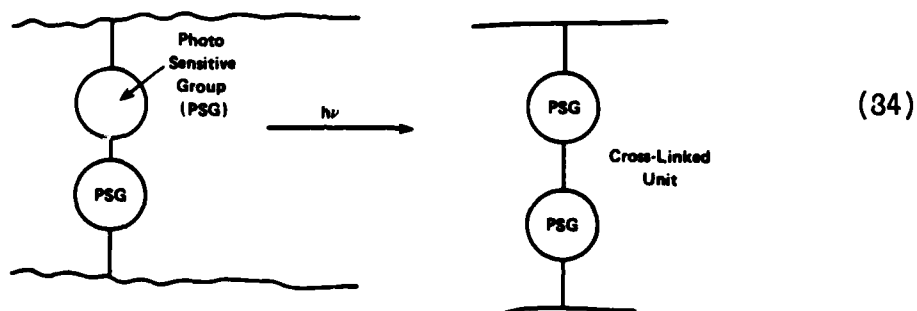
the three stages, the importance of intramolecular reactions, and the applicability of the various theories to the different polymerization stages, such as the classical statistical theories(43,43), the cascade theory(46,47), the percolation theory(48-50), and various kinetic approaches.(51,52)

Simple kinetic considerations show that primary molecules are already formed at very low monomer conversions. Free radical polymerizations reach their steady-state conditions for radical concentrations of approximately 10^{-8} mol/L. If the molar mass of the primary molecules is 10^5 g/mol and if the steady state is exclusively controlled by polymer radicals (which is approximately true for low initiator concentrations), then the steady state is reached for polymer concentrations of 10^{-3} g/L, i.e., at very low monomer conversions.

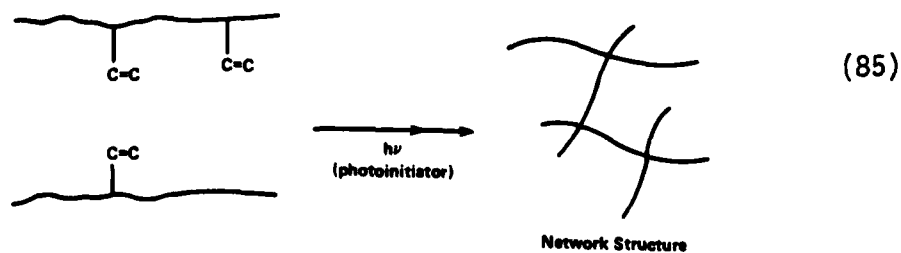
The pendent groups of primary molecules must be already subject to further reactions at these very low monomer conversions, regardless of whether all groups are equally accessible or only a fraction thereof, e.g., the groups on the periphery of the primary macromolecules. Pendent functional groups may be attacked by primary polymer radicals (or by initiator radicals if the initiator concentration is high) and the thus formed branched polymer radicals may add further monomer molecules. Since branching alone does not lead to gelation(43), addition of polymer radicals onto primary polymer molecules and recombination of branched polymer radicals are the two ways to achieve gelation. Other termination steps, such as the disproportionation reaction of polymer radicals or the termination by initiator radicals, neither increase the degree of polymerization nor the probability for intermolecular polymer/polymer reactions. An exception may be intermolecular chain transfer to primary or branched molecules since the newly formed polymer radicals may add further monomer molecules which in turn increases the molar mass. The probability of such transfer reactions is, however, small compared to addition of polymer radicals to primary or branched molecules.

Regardless of the mechanism associated with gelation of multifunctional vinyl unsaturated monomers their rates of conversion (liquid to solid) are usually much greater than single vinyl unsaturated compounds.

Solid-state photoinduced polymeric crosslinking reactions have only been of interest in thin film photoresist technologies, and this concept usually does not involve a propagation reaction in that it is a single-event-related phenomenon:



Combination of the multifunctional unsaturated monomer gelation concepts (initiation, propagation and termination) with solid state photopolymerization reactions should show a dramatic increase in quantum yield for crosslinked site formation.



In this study it was of prime importance to develop a unique photoinitiator system; hence, the preliminary experiments were carried out in a well-characterized single vinyl unsaturated monomer system such as methyl methacrylate.

The actual photosensitive catalyst/polymer systems studied during this phase of the research program involved singlet-triplet (S-T), triplet-triplet (T-T) energy transfer reactions, free radical intermediates and unsaturated (methylmethacrylate) vinyl monomer-polymer substrates.

Two-Photon Triplet Sensitized Photopolymerization Using Dibromoanthracene and Naphthalenesulfonylchloride

It is known from the literature that anthracene derivatives, especially 9,10 dibromoanthracene (DBA), have the unique ability to be excited at 400 nm to a high S_1 state which can then intersystem cross to a relatively high T_2 state followed by radiationless transition to a lower T_1 state (Figure 7). The anthracene derivatives alone are not photoinitiators but when coupled through energy transfer with a different molecule which cannot absorb 400 nm light energy radiation but does have photoinitiation capabilities then a novel binary wavelength photoactive catalyst system can be envisioned.

The first disclosure of the use of energy transfer in the photoinitiation of polymerization reactions was by McGinniss.⁽⁵⁴⁾ In this system, energy transfer reactions between a photochemically excited state donor molecule (photosensitizer) and ground state acceptor molecule (photo or thermal initiator) were used to generate free radical intermediates:

$$[k_t = f(1/n) \text{ and } n = f(\text{monomer/polymer})] \quad (86)$$

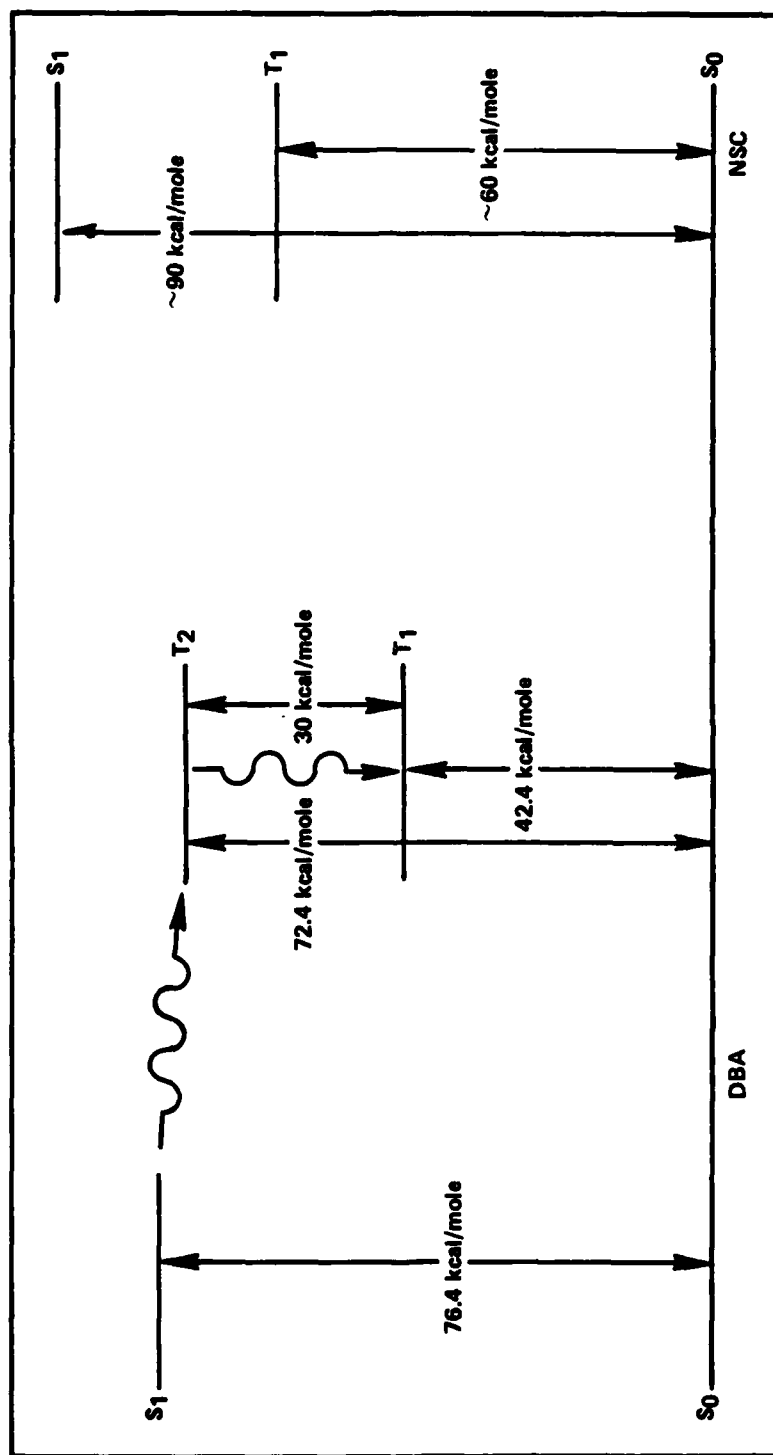
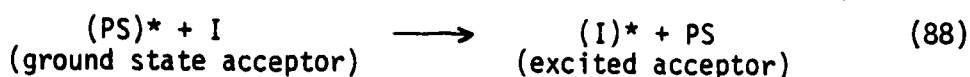
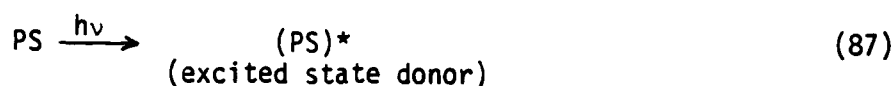


FIGURE 7. ENERGY-LEVEL DIAGRAM FOR 9,10-DIBROMOANTHRACENE (from Reference 2).

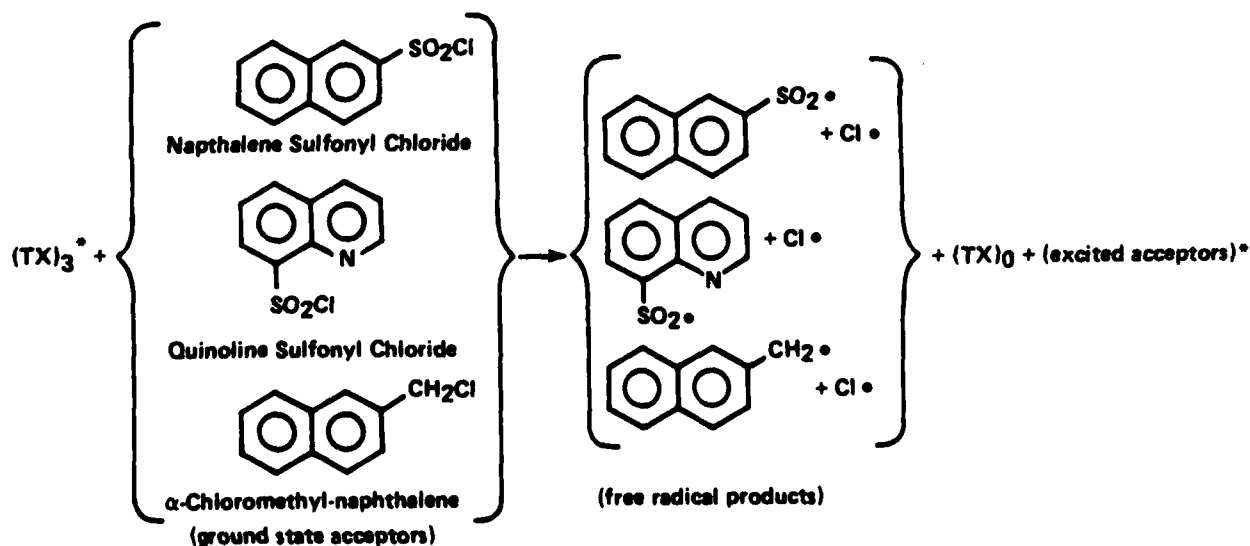
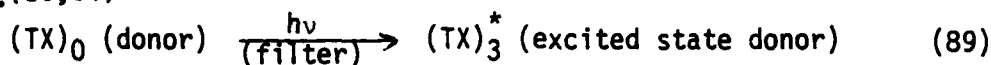


In these systems the photosensitizer does not undergo chemical change, and free radical intermediates are only generated from chemical changes associated with the ground state acceptor molecule (I) during or after the energy transfer process. The photosensitizer (PS) can be an aromatic carbonyl derivative and the initiator (I) can be a photoinitiator (molecules which are capable of undergoing direct photochemical reactions to produce free radicals) or a thermal initiator compound such as the diacyl peroxides, peresters and hydroperoxides; the only requirement for the reaction is that the excited state donor molecule (usually triplet excited state, but a high level excited singlet manifold reaction is also possible) should have a higher energy level value than the ground state acceptor molecule, for efficient transfer of energy.⁽¹⁷⁾

The photosensitized decomposition of benzoyl peroxide with aromatic carbonyl compounds is representative of an energy transfer free radical generation process in that the peroxide (non-light absorbing reaction conditions) is decomposed only in the presence of the photosensitizer (light absorbing species) but without any detectable change in the photosensitizer chemical structure. The ability of the photosensitizer (aromatic carbonyl compounds such as benzophenone, acetophenone, acetophenone, acetophenone) to effect decomposition of benzoyl peroxide depends on the triplet energy levels of the photosensitizer aromatic carbonyl compound. Those aromatic carbonyl compounds having triplet energy values in excess of 55 kcal/mol demonstrate their ability to effect benzoyl peroxide decomposition reactions while those aromatic carbonyl photosensitizers hav-

ing triplet energy levels below 55 kcal/mol do not exhibit this energy transfer free radical generation process.(55)

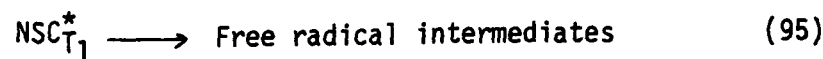
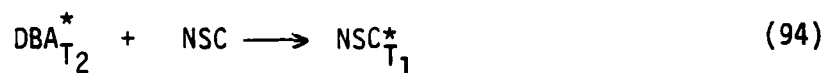
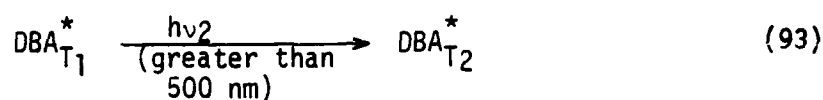
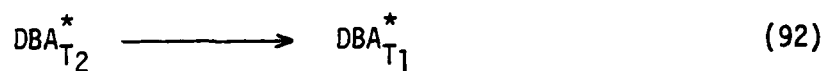
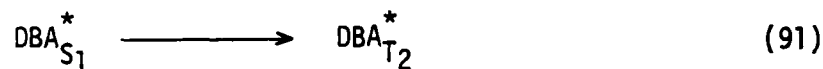
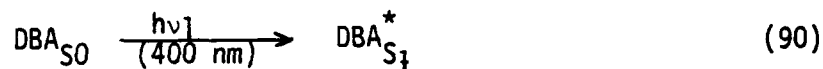
In the following type of energy transfer reaction, thioxanthone (TX) is the only active light absorbing species (cut-off filters or titanium pigments strongly absorb all radiation below 360 nm) contained in the light-filtered reactive monomer system. Thioxanthone alone does not photoinitiate polymerization of vinyl unsaturated monomers. Naphthalene sulfonyl chloride (NSC), chloromethylnaphthalene (CMN) and quinoline sulfonyl chloride (QSC) absorb light at approximately 310-330 nm which results in homolytic cleavage of the sulfonyl chloride bond or chloromethyl bond to produce initiating free radical species, which can in turn effectively polymerize vinyl monomers. In this filtered or pigmented radiation-curable vinyl monomer coating system, all light in the 310-330 nm range is absorbed by the filters or pigment, so direct absorption or excitation by QSC, NSC, or CMN is not allowed. The only way photochemical initiation can take place is through the light absorption of energy (370-380 nm) by TX which can then transfer its absorbed energy to a ground state QSC, NSC, or CMN molecule and result in free radical formation.(15,54)



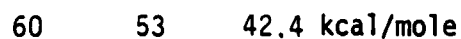
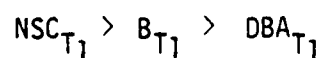
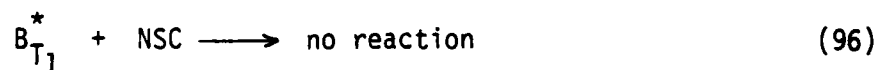
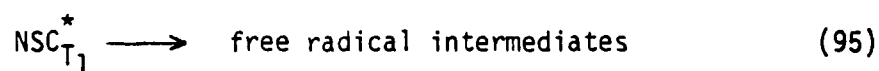
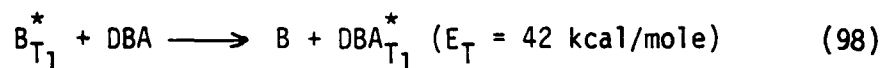
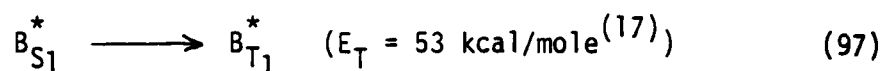
The triplet energy for TX is 65 kcal/mol and the triplet energies for NSC, QSC or CMN are approximately 60 kcal/mol ($E_T = 5$ kcal/mol excess) which meets one of the basic requirements for efficient energy transfer, i.e. E_T of donor (TX) $>$ E_t of acceptor (QSC, NSC, CMN).⁽¹⁷⁾

In this present study the T_1 triplet energy value for NSC ($E_T = 60$ kcal/mole) lies below the T_2 level of DBA [$E_t \approx 72$ kcal/mole⁽²⁾] and above its T_1 level [$E_T = 40$ kcal/mole⁽²⁾]. Only excess energy coming from the T_2 level of DBA can couple with the T_1 level of NSC and cause photoinitiation (Figure 7).

The other major feature of the unique DBA photoactive catalyst systems is its ability to undergo readily allowable $T_1 \rightarrow T_2$ transitions via utilization of a second light source ($\lambda_{\text{max}} > 500$ nm) thus increasing the population of the upper T_2 state (Figure 7). This special feature of DBA allows one to construct a binary wavelength photoactive catalyst system.



Another variation on this concept is the added ability of DBA to be sensitized through its lower level T_1 state through use of another photosensitizer molecule (λ_{\max} 400 nm or greater but with λ_{\max} larger than the ϵ of DBA) having its T_1 level higher than the T_1 level of DBA (Figure 8). A possible mechanistic scheme can be generated as follows, using benzil as a representative photosensitizer:



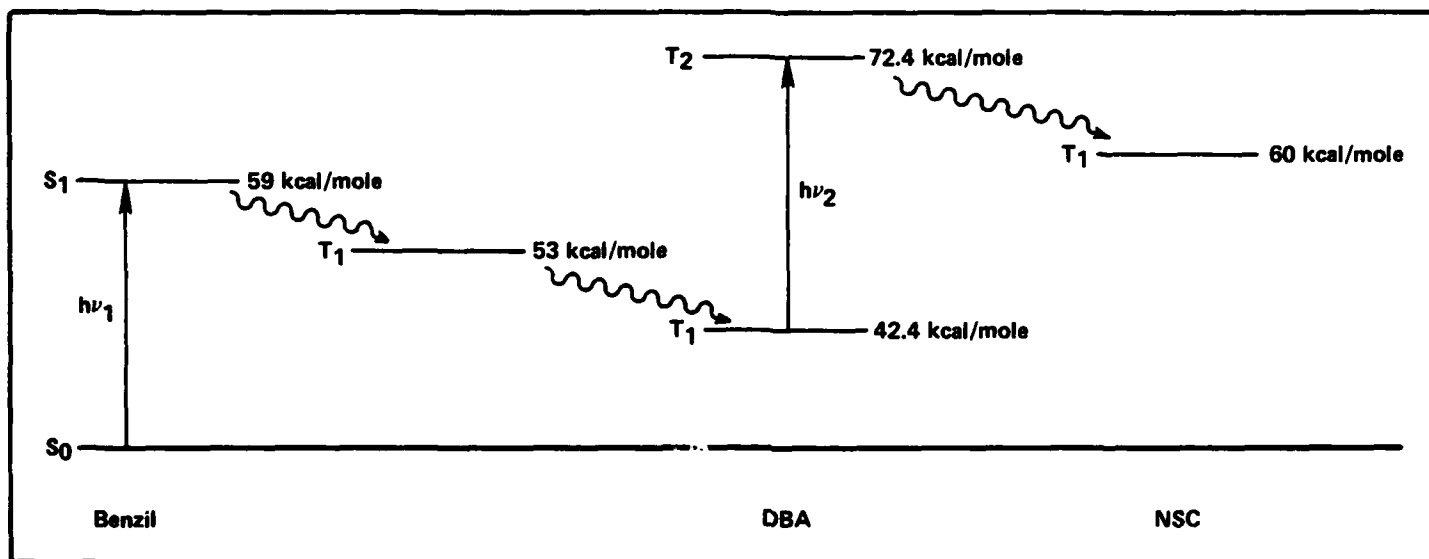


FIGURE 8. SCHEMATIC ENERGY-LEVEL DIAGRAM FOR TRIPLET-SENSITIZED EXCITATION OF DIBROMOANTHRACENE

A major advantage to this scheme is the elimination of the direct $DBA_{S_0} \rightarrow DBA_{S_1}^*$ transition followed by intersystem to DBA_{T_2} and interaction with NSC.

Experimental Details

All chemicals (9,10 dibromoanthracene, 2-naphthalene sulfonyl chloride and 99% methyl methacrylate) were purchased from Aldrich Chemical Company. The naphthalene sulfonyl chloride was recrystallized from chloroform; the inhibitor (65 ppm methoxyhydroquinone) was removed from methylmethacrylate by base extraction and the other materials were used as received. Ultraviolet spectra of the photosensitized monomer solutions were obtained on a Cary 17 and photochemical irradiations (10 ml sample

sizes) were carried out with filtered and nonfiltered Eimac 150 W high pressure Xenon arc lamp light sources. Polymer formation was determined gravimetrically via methanol precipitation of irradiated monomer-polymer solutions. Filters were obtained from the Corning Glass Company.

Key Observations

The concentrations of dibromoanthracene (DBA) and naphthalene sulfonyl chloride (NSC) were adjusted so that the NSC concentration was in excess for efficient energy transfer (Figure 8). DBA does have absorption bands beyond 380 nm, but it was still necessary to include a sharp 410 cut-off filter so that direct absorption of the NSC (λ_{\max} 310 nm) would be prevented (Figure 9). The filter (CS-3-74) does allow about 35% of the light from the source into the 415 nm region, which was sufficient to excite the $S_0 \rightarrow S_1$ transition region of DBA. The results in Table 6 show that unfiltered NSC/MMA solutions polymerize without the benefit of energy transfer from DBA but filtered (CS-3-74) NSC solutions do not produce polymer unless the DBA is present for light absorption and for the $S_1 \rightarrow T_2$ (DBA) $\rightarrow T_1$ (NSC) energy transfer process depicted in Figure 9.

A graphical presentation showing the weight of polymer formed versus exposure time for filtered DBA/NSC/MMA solutions is shown in Figure 10.

The light source used in these experiments had considerable output in the 700 nm to IR wavelength range, and it is possible that readily allowable $T_1 \rightarrow T_2$ DBA transitions could be occurring at the same time as $S_0 \rightarrow S_1 \rightarrow T_2$ DBA and $T_2 \rightarrow T_1$ DBA, thus resulting in a more efficient population of the T_2 DBA state necessary for energy transfer to NSC (T_1 DBA $\ll T_1$ NSC). If any of the excess electronic energy from the T_2 level of DBA fell to the T_1 level of DBA without transferring to the T_1 level of NSC, then this would result in a less efficient photoinitiation process. To test this concept, a combination of filter experiments were carried out in order to isolate certain wavelengths of light energy

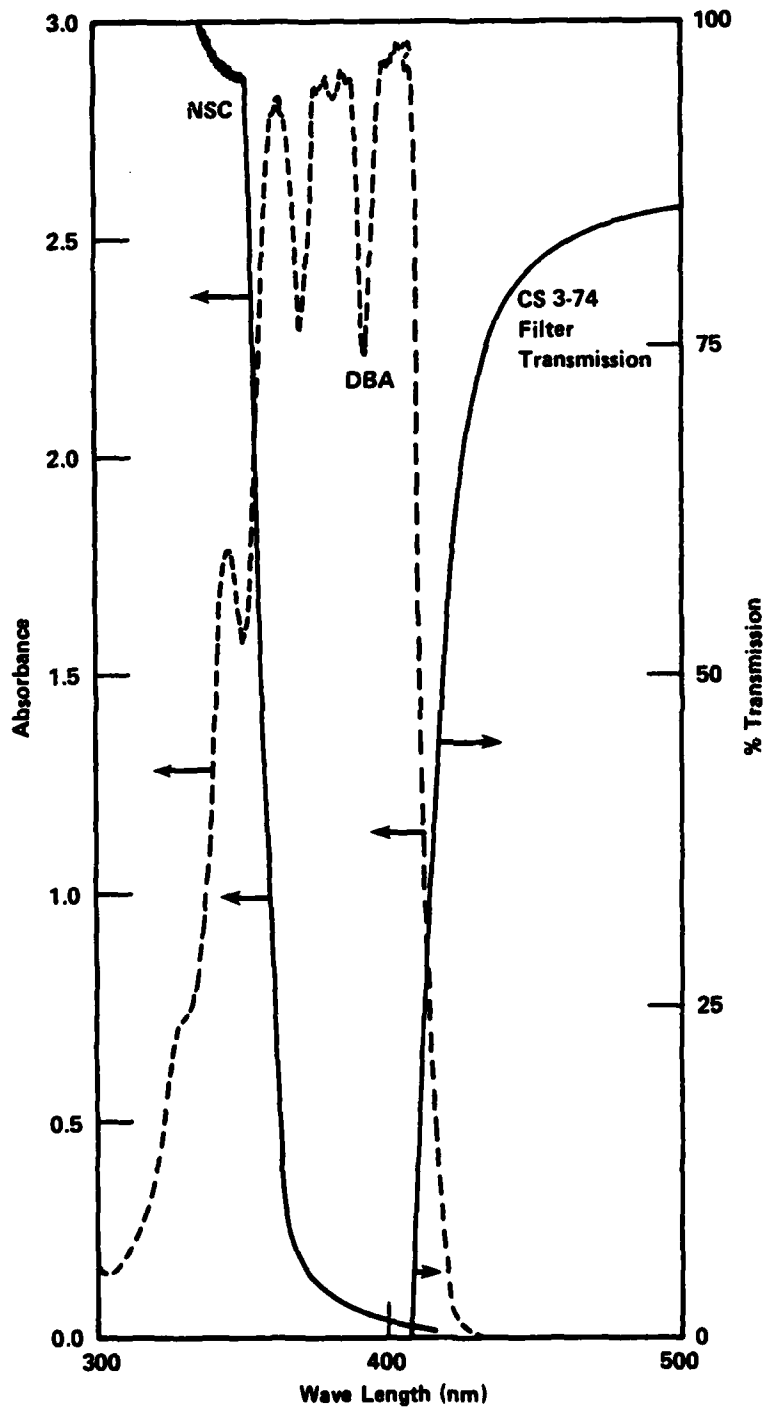


FIGURE 9. EXPERIMENTAL ABSORPTION SPECTRA FOR DBA (dashed line) AND FOR NSC (solid line) IN METHYL METHACRYLATE, SHOWING TRANSMISSION CURVE FOR CORNING CS 3-74 FILTER

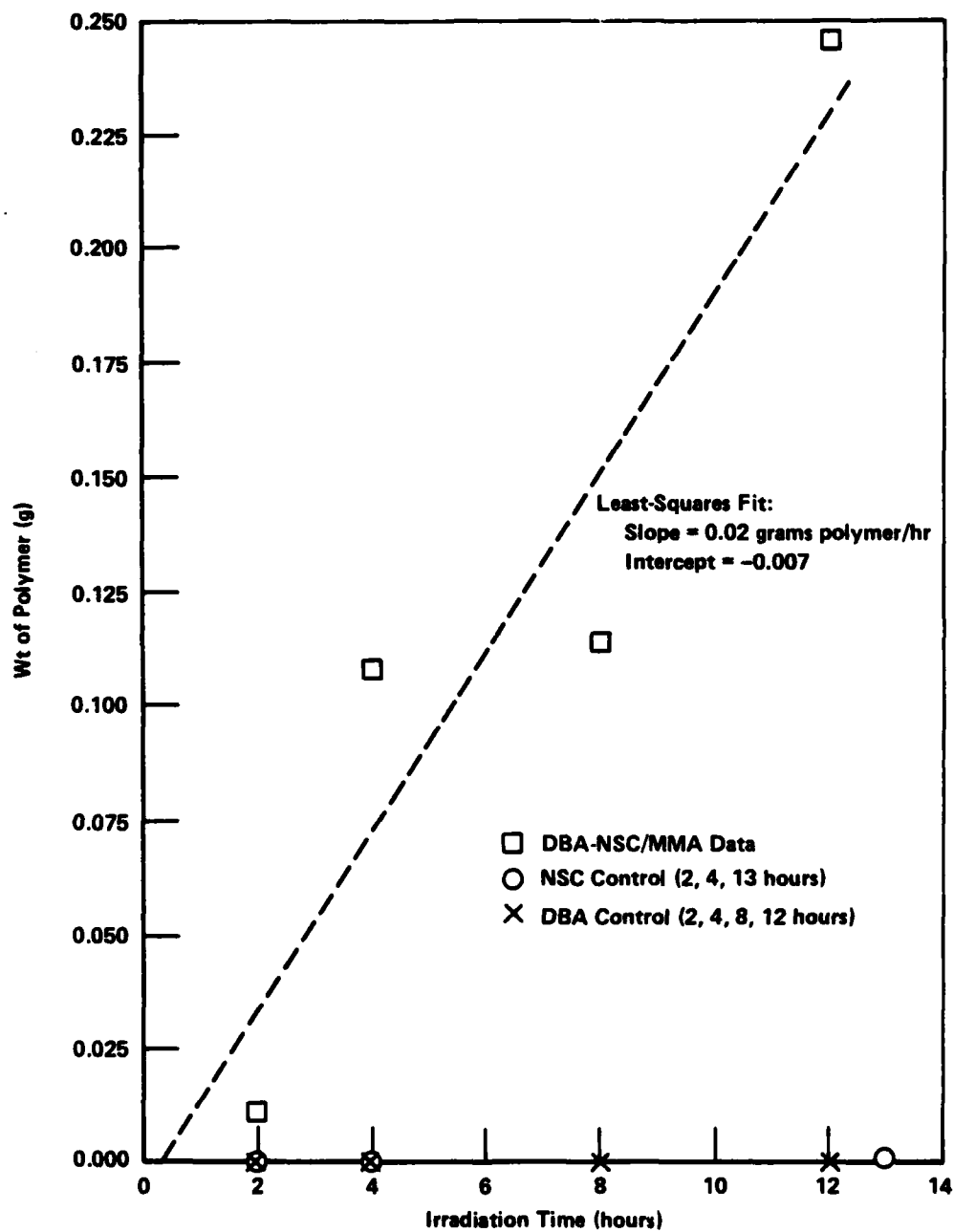


FIGURE 10. PHOTOPOLYMER FORMATION IN THE DBA/NSC/MMA SYSTEM

calculated to excite or prohibit the $T_1 \rightarrow T_2$ DBA transition ($E_T = 30-32$ kcal/mole, 850-900 nm wavelength range). Filter 1 (CS-3-74) cuts off all light below 400 nm but does allow the $S_0 \rightarrow S_1$ DBA transition to occur; Filter 2 (CS-1-59) transmits 380 to 700 nm but has approximately 35% absorption in the IR radiation range; Filter 3 (CS-4-96) transmits 360 to 600 nm and strongly absorbs 660 to 1.5 microns. Monomer samples containing DBA and NSC exposed to the light source containing only filters 1 and 2 ($S_0 \rightarrow S_1 \rightarrow T_2$ DBA $\rightarrow T_1$ NSC and $T_1 \rightarrow T_2$ DBA $\rightarrow T_1$ NSC) showed significant levels of polymer formation in 1 hour. An identical experiment using filters 1, 2 and 3 ($S_0 \rightarrow S_1 \rightarrow T_2$ DBA $\rightarrow T_1$ NSC only and not $T_1 \rightarrow T_2$ DBA $\rightarrow T_1$ NSC) resulted in almost half as much polymer formed in the 1 hour time period as was obtained with filters 1 and 2 (Table 6).

From these experiments one can conclude that the DBA $S_0 \rightarrow S_1$ $T_2 \rightarrow NSC$ T_1 is a viable single-wavelength photoinitiator system, but even more important for this project is the fact that DBA $T_1 \rightarrow T_2$ transitions can be selectively excited to create a very efficient binary wavelength photoactive catalyst system for photopolymerization reactions. A patent disclosure has been written for this facet of the project.

Two-Photon Laser Studies

An important goal of this program is to discover processes that will allow the production of polymeric materials by selectively polymerizing materials at particular points internal to the container surface in which the material to be polymerized resides. Some preliminary experiments run for the production of the selective polymerization of the porphyrin materials with the interaction of two photons will be described in this section of the report. There are two aspects to be discussed in this. First, the experimental rationale and design of the experiments done in this phase will be described. Second, the results of our tests will be given, along with our planned approach for the steps to be taken toward making this two-photon process a reality during the next phase of the program.

TABLE 6. SUMMARY OF DBA/NSC IRRADIATION EXPERIMENTS

MMA	DBA	NSC	Filter 1 CS-3-74	Filter 2 CS-1-59	Filter 3 CS-4-96	Results
+	1%	--	--	--	--	no polymer formed
+	--	2%	--	--	--	polymer formed in 20 minutes
+	1%	2%	--	--	--	polymer formed in 1 hour
+	--	--	--	--	--	no polymer formed
+	0.2%	--	yes	--	--	no polymer formed after 3 hours
+	--	2%	yes	--	--	no polymer formed after 3 hours
+	0.2%	2%	yes	--	--	polymer formed after 3 hours
+	0.2%	2%	yes	yes	--	0.25 gms polymer formed in 1 hour
+	0.2%	2%	yes	yes	yes	0.15 gms polymer formed in 1 hour

By selective excitation of the material with two different wavelengths, it is expected that selective polymerization at a particular spot can be achieved, inside the outer surfaces of the prepolymer. The expectation is that the action of either single wavelength laser will not polymerize the material while the action of the two specified wavelengths will produce the selective energy transitions required to polymerized. It is the goal of this research to develop the knowledge of the material and the steps in the process necessary to produce this selection.

Experimental Design

The excitation of the molecules is made with two lasers with wavelengths specified by the fact that one wavelength will excite the molecule to an upper singlet state. The molecular decay rules are such that many of the molecules will decay through the lowest triplet excited state. The second laser is tuned to excite these molecules into an upper triplet state, above the dissociation limit of the molecule, while not interacting with molecules in the singlet ground state. This process has been summarized in Figures 2 and 3. As described previously a number of preliminary experiments of this type have now been performed using the brominated porphyrin derivatives dissolved in methyl methacrylate (MMA) and in trimethylolpropane triacrylate (TMPTA).

Figure 11 shows the setup of the lasers and the positioning of the material in the system. The laser beams are crossed at their focused position. The beams are focused by quartz lenses at a single spot in the sample cuvette. The beam from the singlet exciting laser is then directed in such a way as to be colinear with the beam from the second laser. The signal is then detected with a photomultiplier observed on an oscilloscope. In this way, the timing of the two signals can be controlled. Strong continuously radiating energy sources could also be used, but pulsed laser sources provide higher upper state populations in controlled periods of time such that the chances for an absorption of the second

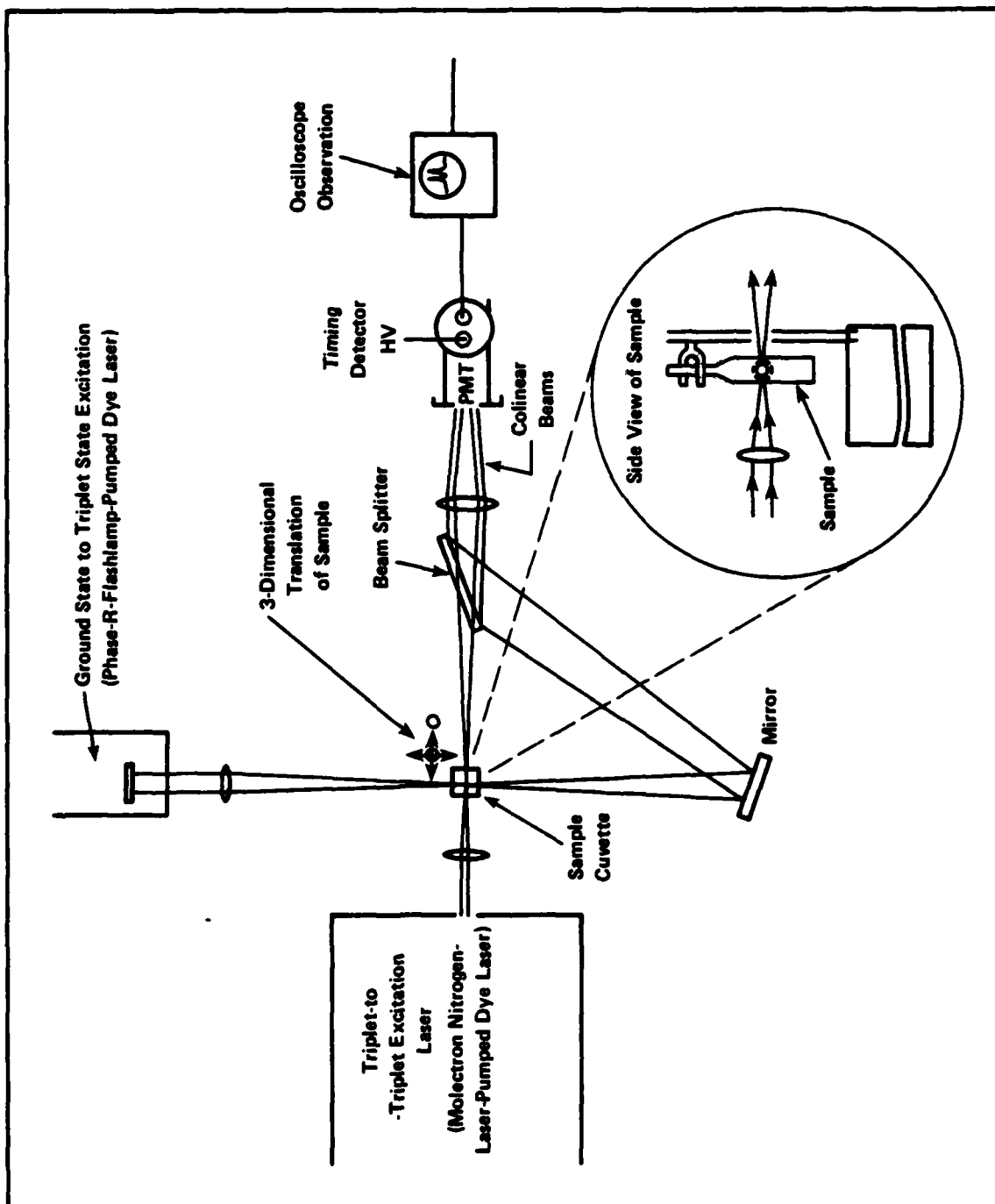


FIGURE 11. ILLUSTRATION OF TWO-BEAM LASER IRRADIATION SYSTEM

wavelength has a higher probability of occurring. Pulsing also reduces the problems associated with heating the samples as compared to a continuous source.

The laser used to excite the porphyrin was a Phase-R DL-1200 V flashlamp-pumped dye laser operating in the 630 nm region of the spectrum. The dye used to produce this excitation was Kiton Red S (5×10^{-3} M in methanol) which was excited as it flowed through the cavity of the flash lamp. The dye was kept cool by means of a circulating fluid temperature controller. The energy of the beam of the exciting laser was about 100 mJ, and had a half width of 2 nm. The energy, the time during the pulse, and the beam cross section determine the intensity of the light which for the Phase-R laser was 8 MW/cm^2 . Data for making calculations can be found in Table 7.

The second laser was a Molelectron UV24-DL14 nitrogen pulsed dye laser which we tuned to 730 nm; this was thought to be optimum for exciting the upper triplet states. The energy of this laser was in the range of 200 microjoules per pulse for the dye Rhodamine B and Oxazine 1 Perchlorate each at a concentration of 5×10^{-3} M (Molelectron Dye 19). The pulse duration of the second laser is only 8 ns, however, and this energy must be controlled in time to arrive at the sample just after the pulse from the first laser. The cross-sectional area of the Molelectron laser beam is also smaller than that from the Phase-R laser. With this data a light intensity of $I = 5 \text{ MW/cm}^2$ is found in the beam during a pulse which is similar to the Phase-R laser. In the case of the porphyrin photoinitiator, the timing of the triplet excitation pulse can be placed any time after 50 ns and up to a few microseconds because the triplet lifetime in the ground state is estimated to be in the tens of microseconds after the first beam has been absorbed.

Considerable effort was needed to synchronize the two systems so that both of the lasers fired at the same time. This was only partially accomplished due to jitter between the two instruments in timing. Figure 12 shows a schematic diagram of the triggering scheme used in our experi-

TABLE 7. DATA ON LASERS AND MATERIALS INTERACTIONS USED
IN TWO-PHOTON EXPERIMENTS ON POLYMERIZATION OF METHYL
METHACRYLATE WITH PORPHYRIN SENSITIZATION

	Laser 1 Phase-R DL1200V		Laser 2 Molelectron UV24-0L14	
Pulse Energy	E_1	100 mJ	E_2	0.2 mJ
Area of Beam	A_{b1}^2	$5 \times 10^{-2} \text{ cm}^2$	A_{b2}^2	$5.0 \times 10^{-3} \text{ cm}^2$
Time of Pulse	τ_1	250 ns	τ_2	8 ns
Repetition Rate (Pulses per Second)		0.33 Hz		0.33 Hz
Wavelength	λ_1	620 nm	λ_2	730 nm
Bandwidth	$\Delta\lambda_1$	$\pm 2 \text{ nm}$	$\Delta\lambda_2$	$\pm 0.1 \text{ nm}$
Effective Optical Path Length at Intersection Point	l_1	0.07 cm	l_2	0.25 cm
Estimated Absorptivity of Porphyrin Sensitizer times concentration	$(\alpha_1 C_1)$	0.2 cm^{-1} at 620 nm	$(\alpha_2 C_2)$	0.4 cm^{-1} at 730 nm

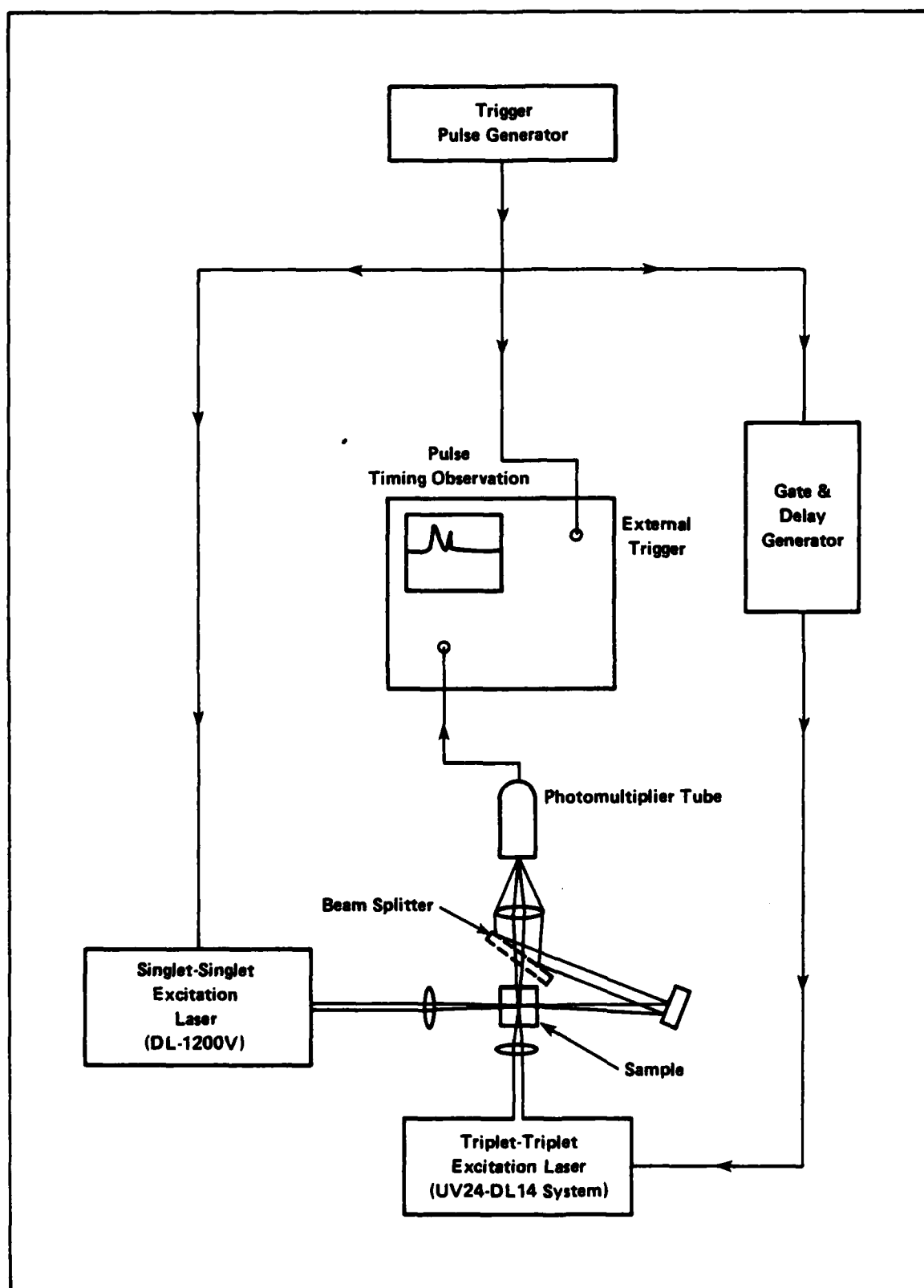


FIGURE 12. SCHEMATIC ILLUSTRATION OF LASER TRIGGERING SCHEME

ments to control this timing. By varying the delay in the trigger of the Molelectron laser, the laser outputs of the two could be synchronized. The Molelectron output seemed steady within 20ns as compared to the trigger input driving the two systems. The Phase-R laser seemed to jitter in a distribution around the Molelectron laser by as much as 1-2 microseconds. We estimate that this effect substantially reduced the number of shots in which the two lasers were actually synchronized in time. Improvements in the triggering of the Phase-R laser will enable this jitter to be reduced to a great extent in the next phase of the program. A second limitation of the equipment was the extremely low number of pulses that could be generated during a run. The Phase-R laser can only pulse about once every three seconds, while the Molelectron can typically pulse up to 30 pps without much loss in energy per pulse. We anticipate that this situation will be remedied by the acquisition of an improved flashlamp for the Phase-R laser during the next few months.

Experimental Results and Expected Direction of Research

The experiments done to date are summarized in this section. First, the solution of porphyrin material in monomer was placed in the cuvette and degassed, either by freeze-pump-thaw cycles under vacuum or by purging with a flow of argon gas for 15-30 minutes. The sample was then placed in the focused intersection of the two beams as described above. The lasers were then triggered for 5 minutes, and the sample observed again. This process was then repeated for varying time periods of up to an hour or two in some cases. The lasers were fired at time intervals of three seconds, as limited by the repetition rate of the Phase-R laser. The Phase-R laser also had a tendency to lose pulse energy after only a few minutes of operation; this may have been due to the dye becoming depleted through use, or more likely, because the transfer of heat energy to the cooling unit was not taking place rapidly enough. This would result in temperature gradients being set up in the dye solution, reducing its

output. The dye was periodically allowed to "rest" for about 1 hour after every 20 minutes of operation, so the experiments were often quite time-consuming to conduct.

For most of the experiments done with MMA solutions, little if any polymer formation could be observed directly after these irradiations. This is most likely because the MMA crosslinks relatively inefficiently, and any polymer formed was still dissolved in the monomer. The presence of polymer in many of the runs was confirmed by diluting the irradiated solutions with methanol, which precipitated the polymerized material. This approach was clearly unsatisfactory for the formation of solid objects with precise shape, however.

Most recent experiments in this series have been carried out using trimethylolpropanetriacrylate (TMPTA), rather than MMA. TMPTA is a highly effective crosslinking monomer, and it was felt that this would give more realistic assessments of the performance of the various photo-initiators that were being developed. Indeed, polymerization was observed frequently in these systems, with a primary problem being that now the polymerization was too rapid. In a number of experiments, it appears that the polymerization process propagated out of the irradiated zone, giving rise to large "blobs" of polymer. These results demonstrate conclusively that the two-beam process can be made to work with laser irradiation, but clearly much remains to be learned about the control of the process. Our experiments during the coming year will be directed toward this goal.

Estimated Amount of Polymerization Expected from Two-Beam Laser Experiments

An approximate calculation of the amount of polymerized material we are likely to form can be done using some material assumptions along with the data on the lasers and materials which were summarized in Table 7. These data were compiled from measurements made on our system in several different experiments. It must be noted, however, that the pulse energy

varies with time, and the actual pathlength for beam 2 is very difficult to measure. Therefore, this calculation should be regarded as an estimate rather than as an accurate prediction. In future experiments, more of these parameters will be measured carefully, so as to make future calculations more accurate.

In order to do these calculations on polymerization we must first characterize the laser beams at their intersection point: Their pulse energies are different and their cross sectional areas and times of lasing of the beams are also different. The times of interest are the times during which the beams are lasing and affecting the sample. This gives the intensity during firing:

$$I = \frac{E}{\tau A} \quad (99)$$

where the symbols are as defined in Table 7 for each laser

For the Phase R-laser, $I = 8.0 \text{ MW/cm}^2$

For the Molelectron laser, $I = 5.0 \text{ MW/cm}^2$

The Phase-R laser fires for a much longer pulse duration than the Molelectron laser, so the total amount of energy put into the sample is larger for the first laser. Since the porphyrin material is expected to have a lifetime in this system of tens of microseconds, we would like to set the timing of the second pulse to occur 250 ns after the first pulse. In this way, we take advantage of the full effect of the first beam, and yet relatively few of the excited sensitizing molecules will have decayed to the ground state. The relationship between the number of photons available and beam energy is just

$$E = \frac{Nhc}{\lambda} \quad \text{or} \quad N = \frac{E\lambda}{hc} \quad (100)$$

where E is the beam pulse energy

λ is the beam wavelength

h is Planck's constant (6.62×10^{-34} j-s)

c is the speed of light

N is the number of photons

This gives $N_{p1} = 3.17 \times 10^{17}$ photons from the Phase-R laser. Not all of N_{p1} are effective, however, because only 35% of the photons cross through the volume of beam 2 as shown in Figure 13.

Effectively,

$$N_{p1} = 1.1 \times 10^{17} \text{ photons/pulse}$$

$$N_{p2} = 7.4 \times 10^{14} \text{ photons/pulse}$$

Using Beer's Law relationship we can get an estimate of the number of molecules excited to the S1 state, as shown in Equation (101).

$$\ln \left(\frac{I_1}{I_2} \right) = (\alpha_1 C_1) \ell_1 \quad (101)$$

where

I_1 is the original intensity,

I_2 is the transmitted intensity,

ℓ_1 is the length of beam 1 in the crossed beam volume, and

$(\alpha_1 C_1)$ is the product of the absorption cross section times the concentration of the sensitizer. (α is base e)

This last quantity, $\alpha_1 C_1$, has been determined to be 0.2 cm^{-1} at the position of excitation. The wavelength of choice is at a position which allows absorption but not so much absorption that the beam is appreciably absorbed between entering and leaving the cuvette. For this case

$$\left(\frac{I_1}{I_2} \right) = 0.8 \text{ through the cuvette} \quad (102)$$

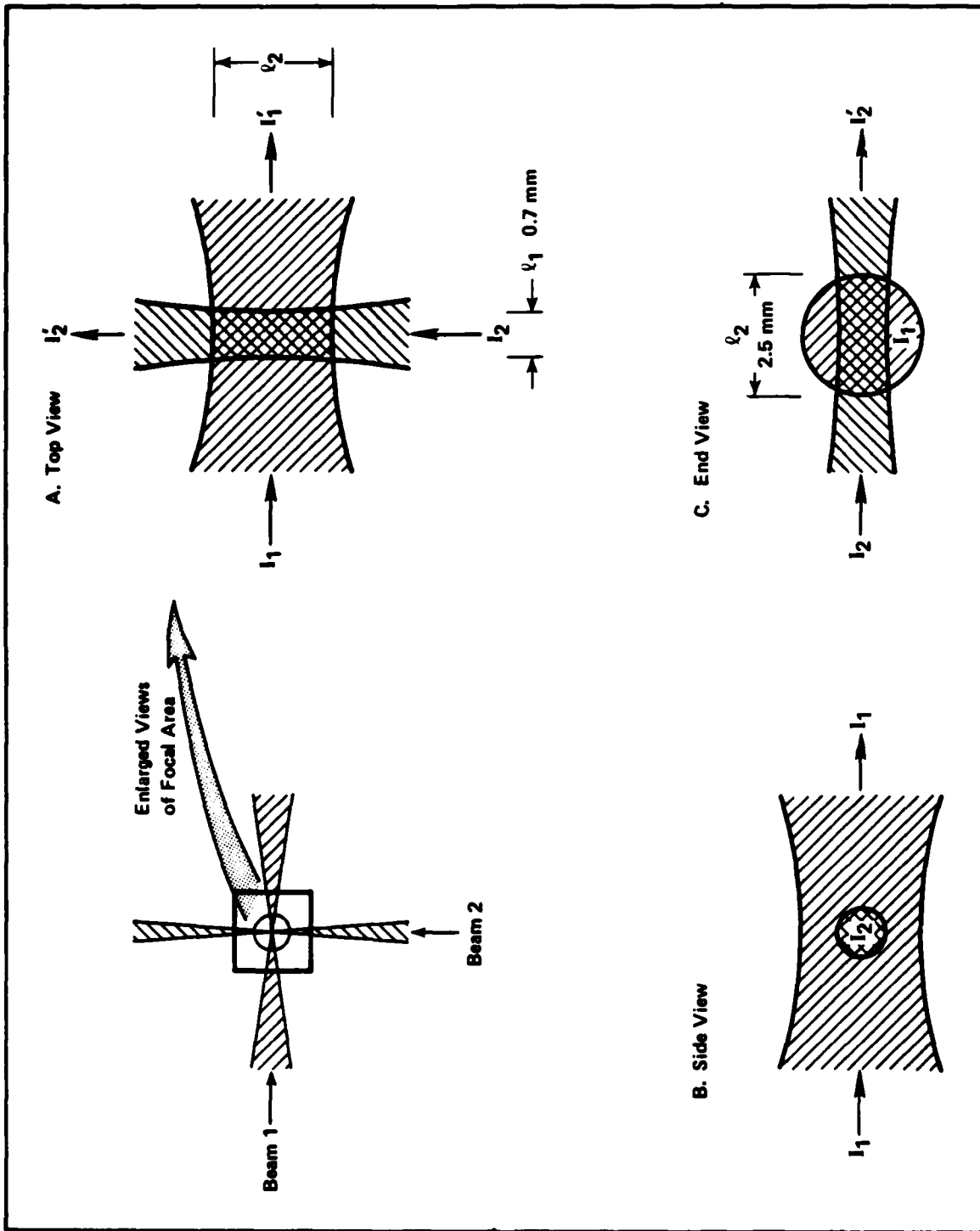


FIGURE 13. VIEWS OF FOCUSED BEAM INTERSECTIONS

The fraction of photons that send molecules to the S_1 state from the ground S_0 state is $(1-T)$ where T is the transmittance, I'/I .

$$(1-T) = (1 - \frac{I'}{I}) \quad (103)$$

$$= (1 - \exp(-\alpha_1 C_1 l_1)) \quad (104)$$

$$= 0.014$$

Therefore, $M_{S_1} = (1-T) N_{p_1} \quad (105)$

where N_{p_1} is the number of photons in the pulse of laser 1.

$$M_{S_1} = 1.5 \times 10^{15}/\text{pulse} \quad (106)$$

We estimate 80% of these go the triplet state

$$M_{T_0} = 0.8 M_{S_1} = 1.2 \times 10^{15}/\text{pulse} \quad (107)$$

To estimate the number of excited S_1 molecules that go to the upper triplet state we must know what is relative concentration C_3 is present as compared to C_1 and make an estimate of α_3 . By knowledge of the available molecules for absorbing the original beam and the volume in which this interaction takes place, we can estimate the number of molecules in the ground state in the beam intersection. The data are as follows:

Volume Sample (V)	= 3 ml
Sample Density (ρ)	= 0.85 gm/ml
Molecular Weight, W	= 90 (Molecular weight of the Methyl Methacrylate)
Available Material	= 2.55 gm
	= 0.028 moles
	= 1.75×10^{22} molecules of MM

Sensitizer Concentration in MMA = 10^{-3} moles/liter

$$M_{S_0} = (\text{Beam Volume})(\text{Relative Sensitizer Concentration}) \\ (\text{MMA molecules/cm}^3)$$

$$M_{S_0} = 5.7 \times 10^{15} \text{ molecules}$$

This indicates that the triplet state concentration after the original pulse is about 20% of the original concentration of sensitizer molecules on the MMA. α_3 is chosen to be close to what we hope is the peak of the triplet absorbance which we estimate to be $\sim 8X$ stronger than the absorption band edge which was used for the excitation in the ground state. We need not worry about absorbance in the sample at any point but the intersection point because no molecules in the path of the second laser are in the triplet state except at that point. In contrast, the singlet excitation must occur at a point where some, but not too much, absorption will occur. Hence, the need for excitation away from the absorption band maximum.

$$\text{Therefore,} \quad \alpha_3 C_3 = 0.4 \quad (108)$$

Using the same method as with M_{S_1} , M_{T_1} can be calculated with $z = 0.2$ cm, using Beer's law:

$$\begin{aligned} M_{T_1} &= (1 - T_3) (N_{p2}) \\ &= (1 - 0.9) (7.4 \times 10^{14}) \\ M_{T_1} &= 7.4 \times 10^{13} \end{aligned} \quad (109)$$

where T_3 is the transmittance and N_{p2} is the number of photons from the second laser.

where M_{T1} is the number of molecules in the excited triplet state after the second laser fires. It is assumed that 50% of these molecules, M_I , become dissociated, so $M_I = 4 \times 10^{13}$. We estimate that the number of linking events per dissociated molecule is approximately 500, based on previous experience. Therefore, we can say that the number of crosslinks initiated, M_C , is approximately

$$M_C = 2 \times 10^{16} \text{ events per pulse.} \quad (110)$$

In our experiments, up to 10,000 synchronized pulses were fired, but because of jitter and loss of output power near the end of the dye lasing periods we feel have effectively seen about 5000 effective pulses. Linking this with the typical conditions of the sample,

$$\text{Percent of Molecules} = \frac{100 (\text{Number of Pulses})(\text{Molecules Linked per pulse})}{(\text{Number of Molecules Available to Line})}$$

$$= 0.5 \% \quad (111)$$

Thus, we should have polymerized about 0.5% of the material in our sample under the conditions assumed for this estimate. While this may not have been detectable for the MMA system, because of the solubility of the polymer, the results in TMPTA suggest that this estimate is conservative; at least, in those experiments, up to 10% of the sample was polymerized in a much shorter time.

SUMMARY OF FUTURE PLANS

It is clear that the research performed to date has succeeded in identifying a number of the key parameters which govern the behavior of a photochemical machining system, and that several promising photoinitiator systems have been developed. It is also clear, however, that much improvement must be realized before a useful system will have been developed.

The strengths of the laser irradiation system we have assembled are the tunability of the system (by changing dyes and by scanning wavelengths with the second laser) and the reasonably high peak powers that can be obtained. Improvements will be made in a number of operating parameters that should raise yields in the materials we are presently working with. Experiments on other material systems are planned also, notably with sulfonyl chloride initiators based on rubrene and on tetraphenylporphyrin.

The following problems will be addressed while making experimental improvements for our studies during the next several months:

- Attempt to eliminate temperature gradients in dye and temperature increases in dye of Phase-R laser. This would increase the power and number of pulses available from this laser.
- Remove the jitter in the Phase-R laser to optimize constant time delays in the firing of the two lasers.
- Increase the power of the Molelectron laser by a factor of 1.5 or better.
- Focus the beams to smaller volumes so the polymerization occurs in a more concentrated volume.
- Reduce sample size so that a higher fraction of the material will be successfully polymerized.
- Increase the flexibility of focusing on the beam intersection

- Increase the flexibility of focusing on the beam intersection spot with movable mounts to increase accuracy in beam overlap.
- Investigate new rubrene- and porphyrin- based sulfonyl chloride initiators in a variety of new polymer systems, so as to obtain better spatial resolution of crosslinking.

We remain both enthusiastic and optimistic that these problems can be solved successfully, and we look forward to the emergence of three-dimensional photochemical machining as a truly viable aid to the design and prototyping of precision castings.

REFERENCES

1. Labhart, H. and Heinzelmann, E., in "Organic Molecular Photophysics", Vol. I, J. B. Birks, Ed., John Wiley and Sons, London, England (1973), Chapter 6.
2. (a) Liu, R.S.H. and Gale, D. M., J. Amer Chem. Soc., 90, 1897 (1968);
(b) Liu, R.S.H., ibid., 90, 1900 (1968).
3. Yildiz, A., et al, J. Chem. Phys., 49, 1403 (1968).
4. Tsvirho, M.P., et al, Opt. Spectrosc., 34, 635 (1973).
5. Sapunov, V.V., et al. Zh. Prikl. Spektrosk., 21, 667 (1974).
6. The preparation of rubrene dibromide is described by Keszthelyi, C. P. and Bard, A. J., J. Org. Chem., 39, 2936 (1974).
7. Oster, G. and Yang, N. L., Chem. Reviews, 68, 125 (1968).
8. Kinstle, J. F., Paint Varn. Prod., 63 (6), 17 (1973).
9. Labana, S. S., J. Macromol. Scis. Reviews in Macromolecular Chemistry, 11(2), 299 (1974).
10. Pappas, S. P., Progr. Org. Coatings, 2 (4), 333 (1974).
11. Rabek, J. F., Photochem. Photobio., 7, 5 (1968).
12. Pappas, S. P. and McGinniss, V. D., in: "UV Curing Science and Technology", Pappas, S. P., Ed., Technology Marketing Corp., Connecticut, USA (1975).
13. Amivi, S. M., Bamford, C. H. and Mullik., J., J. Poly. Sci., Poly. Symp., 50, 33 (1975).
14. McGinniss, V. D., SME technical paper, FC76-486 (1976).
15. McGinniss, V. D., Photographic Science and Engineering, 23 (3), 124 (1979).
16. Rabek, J. E., Photopolymers - Principles, Processes and Materials, Technical papers, SPE, Mid-Hudson Section, October, No. 27 (1973).
17. Turro, N. J., Modern Molecular Photochemistry, Benjamin/Cummings, California, USA (1978).
18. Knowles, A., Chemistry and Industry, 17, 1058 (1973).

19. McGinniss, V. D., J. Radiation Curing, 2, 3 (1975).
20. Cohen, S. G., Parola, A. and Parsons, G. H., Chem. Reviews, 73, 141 (1973).
21. Rust, J. B., "Photopolymers - Principles, Processes and Materials," Technical papers, SPE, Mid-Hudson Section, October, No. 55 (1970).
22. Rollefson, G. K. and Burton, M. (Eds.), "Photochemistry and the Mechanism of Chemical Reactions," Interscience, New York, N.Y. (1942).
23. Jenkins, A. D. and Ledwith, A. (Eds.) "Reactivity, Mechanism and Structure in Polymer Chemistry", John Wiley, New York, N.Y. (1974).
24. Leermakers, P. A. and Weissberger, A. (Eds.) Technique of Organic Chemistry, Vol. XIV, Interscience, New York (1969).
25. Turro, N. J., Chem. Eng. News, 45, 8 (1967).
26. Cundall, R. B., J. Oil Col. Chemists Assoc., 59, 95 (1976).
27. Wells, C.H.J., "Introduction to Molecular Photochemistry," Chapman and Hall, London (1972).
28. Simons, J. P., "Photochemistry and Spectroscopy", Wiley-Interscience, London (1971).
29. Hulme, B. E., Paint Manufacture, 9, March (1975).
30. (a) Murov, S. L. (Ed.), Handbook of Photochemistry, Marcel Dekker, New York (1973),
(b) Heine, H. G. and Trankneker, H. J., Progr. Org. Coatings, 3, 115 (1975).
31. (a) McGinniss, V. D., Provder, T., Kuo, C. Y., and Gallopo, A., Macromol., 11, 405 (1978).
(b) Jaffe, H. H. and Orchin, M. (Eds.), "Theory and applications of Ultraviolet Spectroscopy", John Wiley, New York, N.Y. (1966).
32. Labana, S. S., "Ultraviolet Light Induced Reactions in Polymers", ACS Symposium Series 25 (1976).
33. Calvert, J. G. and Pitts, J. N., Jr., Photochemistry, John Wiley, New York, N.Y. (1966).
34. Schnabel, W., Photographic Science and Engineering, 23 (3), 154 (1979).
35. DeSchryver, F. C., Pure Appl. Chem., 34, 213 (1973).

36. Delzenne, G., *Ind. Chim. Belg.*, 24, 739 (1959)
37. Delzenne, G., *Ind. Chim. Belg.*, 30, 679 (1965).
38. Hutchison, J. and Ledwith, A., *Advances in Polymer Science*, 14, 49 (1974).
39. Rudolph, H., Rosenkranz, H. J. and Heine, H. G., *ACS Polymer Preprints*, 16 (1), 399 (1975).
40. McGinniss, V. D. and Dusek, D. M., *J. Paint Technol.*, 46 (589), 23 (1974).
41. Carothers, W. H., *Chem. Rev.*, 8, 402 (1931).
42. See, e.g., Aso, C., Kunitake, T., and Tagami, S., *Prog. Polym. Sci. Jpn.*, 1, 149 (1971); Corfield, G. C., *Chem. Soc. Rev.*, 1, 523 (1972); Butler, G. B., Corfield, G. C., and Aso, C., *Prog. Polym. Sci.*, 4, 71 (1975).
43. Flory, P. J., *J. Am. Chem. Soc.*, 63, 3083, 3091, 3096 (1941); *J. Phys. Chem.*, 46, 132 (1942); *Principles of Polymer Chemistry*, Cornell University Press, Ithaca, New York, 1953.
44. Stockmayer, W. H., *J. Chem. Phys.*, 11, 45 (1943); 12, 125 (1944).
45. Walling, C., *J. Am. Chem. Soc.*, 67, 441 (1945).
46. Gordon, M., *Proc. R. Soc. London, Ser. A*, 268, 240 (1962); Dobson, G. R. and Gordon, M., *J. Chem. Phys.*, 41, 2389 (1964); 43, 705 (1964); Butler, S., Gordon, M., and Malcolm, G. N., *Proc. R. Soc. London, Ser. A*, 295, 29 (1966); Gordon, M. and Scantlebury, G. R., *J. Polym. Sci., Part C*, 16, 3933 (1968); Gordon, M., Kucharik, S., and Ward, T. C., *Collect. Czech. Chem. Commun.*, 35, 3252 (1970).
47. Dusek, K. and Ilansky, M., *J. Polym. Sci., Polym. Symp.*, 53, 57, 75 (1977).
48. Hammersley, J. M., *Proc. Cambridge Philos. Soc.*, 53, 642 (1957).
49. Kirkpatrick, S., *Rev. Mod. Phys.*, 45, 574 (1973).
50. Stauffer, D., *J. Chem. Soc., Faraday Trans.*, [2] 72, 1354 (1976).
51. Gordon, M., *Proc. R. Soc. London, Ser. A*, 201 569 (1951); *J. Chem. Phys.*, 22, 610 (1954).
52. Soper, B., Haward, R. N., and White, E.F.T., *J. Polym. Sci., Polym. Chem. Ed.*, 10, 2545 (1972).

53. Kast, H. and Funke, W., Makromol. Chem., 180, 1335 (1979).
54. McGinniss, V. D., in "Ultraviolet Light Induced Reactions in Polymers", S. S. Labana, Ed., ACS Symposium Series No. 25, American Chemical Society, Washington, DC (1976), p. 135.
55. (a) Farenholtz, S. R. and Trozzollo, A. M., J. Amer. Chem. Soc., 93, 251 (1971);
(b) Walling C. and Gibian, M.J., ibid, 87, 3413 (1965).